Tempestite frequency curves: a key to Late Ordovician and Early Silurian subsidence, sea-level change, and orbital forcing in the Anticosti foreland basin, Quebec, Canada

D.G.F. Long

Abstract: Following partial closure of the northern Iapetus Ocean along the Newfoundland segment of the St. Lawrence Promontory, subsidence along the Anticosti Platform was influenced by residual thermal subsidence, renewed tectonic loading by thrust sheets to the south, and sediment loading. Basement subsidence, calculated by removing the effects of sediment loading, was between 2 and 5 cm/ka in the Caradocian, increasing to 8.6 cm/ka in the Pusgillian and Cautleyan, and reaching a maximum of 17.7 cm/ka in the Rawtheyan, during deposition of the Princeton Lake and Vauréal Formations. A marked decline in subsidence, beginning in the Hirnantian and continuing into the Early Silurian, may reflect decoupling of thrust loads to the south, although a further stage of thrust loading may have occurred in the Aeronian during deposition of the lower part of the Jupiter Formation. Storm frequency curves, produced using tempestite abundance, thickness, and grain size through more than a kilometre of carbonate strata on Anticosti Island, allow recognition of long period, 3rd-order trends. These are in part similar to local sea-level trends deduced from direct interpretation of sedimentary structures, but depart significantly from paleontological-based sea-level curves. Shorter period 4th-order cycles appear to be related to orbital eccentricity with periods of 100 and 400 ka. These may reflect periods with falling sea levels, increasing storm activity, or enhanced sediment flux to the middle and outer shelf.

Résumé : Après la fermeture partielle de l'océan Iapetus Nord le long du segment terre-neuvien du promontoire du Saint-Laurent, la subsidence le long de la plate-forme d'Anticosti a été influencée par la subsidence thermique résiduelle, le renouvellement du chargement tectonique par des nappes de charriage vers le sud et les charges exercées par les sédiments. La subsidence du socle, calculée en soustrayant les effets du chargement par les sédiments, était de 2 à 5 cm/ka au Caradocien; elle a augmenté à 8,6 cm/ka au Pusgillien et au Cautleyan et atteint un maximum de 17,7 cm/ka au Rawtheyen, lors de la déposition des formations de Princeton Lake et de Vauréal. Un déclin marqué de la subsidence, débutant au Hirnantien et se prolongeant au Silurien précoce, pourrait être le reflet du découplage des charges des nappes vers le sud, bien qu'un étage de renouvellement des charges des nappes puisse avoir eu lieu à l'Aéronien durant la déposition de la partie inférieure de la Formation de Jupiter. Les courbes de fréquence des tempêtes, basées sur l'abondance des tempestites, l'épaisseur et la granulométrie le long de plus d'un kilomètre de strates de carbonates sur l'île d'Anticosti, permettent de reconnaître des tendances de longues périodes du 3e ordre. Ces tendances sont en partie semblables aux tendances du niveau local de la mer déduites de l'interprétation directe des structures sédimentaires, mais elles diffèrent significativement des courbes du niveau de la mer établies à partir de données paléontologiques. Des cycles plus courts, du 4e ordre, semblent être reliés à excentricité orbitale avec des périodes de 100 à 400 ka. Ces cycles pourraient être le reflet de baisses du niveau de la mer, d'un accroissement du nombre de tempêtes ou d'un apport accru de sédiments sur la plate-forme moyenne et externe.

[Traduit par la Rédaction]

Introduction

Paleozoic strata exposed on Anticosti Island, Quebec, Canada, were deposited as part of a periodically storm-influenced equatorial carbonate ramp to platform sequence, in a foreland basin setting along the western margin of the Iapetus Ocean (Long 1997; Cousineau and Longuépée 2003; Lavoie et al. 2003). The exposed Ashgill (Rawtheyan, possibly Cautleyan) to Llandovery (Telychian, and possibly earliest Wenlockian) succession consists predominantly of grey to light brown, richly fossiliferous limestone and mudstone with minor amounts of siliciclastic clay and sand. It includes one of the most complete sections in the world across the Ordovician–Silurian boundary (Barnes 1988), serving as an alternative boundary stratotype, in a shallow-shelf setting, to the graptolitic, deeper water stratotype at Dob's Linn, Scotland (Underwood et al. 1997). Minor patch reef complexes are present within the Anticosti succession (Copper 1989),

Received 29 December 2005. Accepted 30 August 2006. Published on the NRC Research Press Web site at http://cjes.nrc.ca on 3 May 2007.

Paper handled by Associate Editor M. Gibling.

D.G.F. Long. Department of Earth Sciences, Laurentian University, Sudbury, ON P3E 2C6, Canada (e-mail: dlong@laurentian.ca).

 doi:10.1139/E06-099

Fig. 1. Distribution of Ordovician and Silurian strata on Anticosti Island. Insert shows position of Anticosti at about 444 Ma.

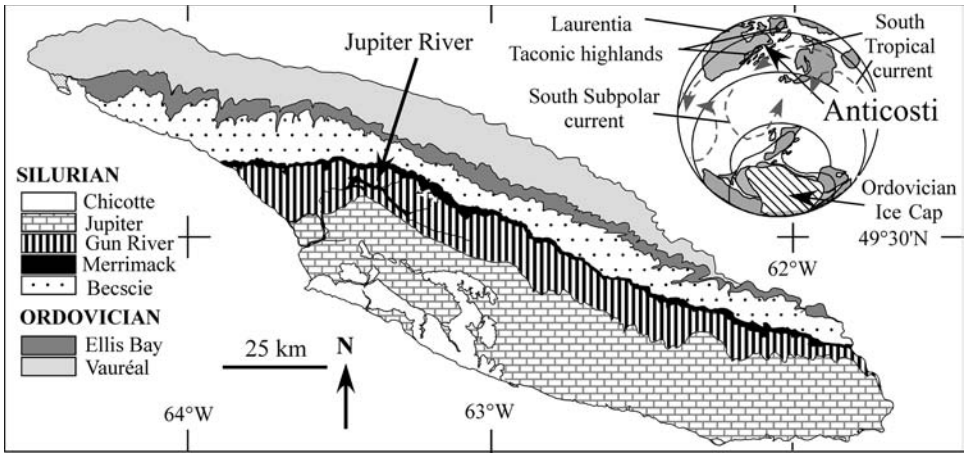

with minor erosional gaps around some of these reefs attributed to storm-enhanced subtidal erosion. Siliciclastic-rich strata are rare and occur primarily in the eastern outcrops (Copper and Long 1989, 1990; Long and Copper 1994; Long 1997).

The objective of this paper is first to provide a brief description of the lithology and sedimentology of the succession, as previously this information was largely restricted to field guides. This information is then used to determine the relative influence of load-induced subsidence and sea-level change. By combining bed-by-bed information from numerous detailed surface and subsurface sections, an attempt is made to determine whether tempestite frequency analysis can be used to determine whether the relative abundance of storm-induced event beds corresponds to predicted global changes in eustatic sea level and (or) predicted Milankovitch-style orbital cyclicity. Dates used in this paper follow Cooper and Sadler (2004) and Melchin et al. (2004).

Stratigraphy

The exposed Paleozoic succession on Anticosti Island has been divided into seven formations (Fig. 1), with five additional formations recognized in the subsurface (Fig. 2). These are cut by tholeiitic dikes of Jurassic age (not shown) along the north-central part of the island (Bédard 1992; Pe-Piper and Piper 1999). Individual formations exposed at the surface are described in the following subsections. More comprehensive descriptions, with details of the paleontology, are provided in papers and field-guides by Long and Copper (1987*a*, 1987*b*, 1994), Copper and Long (1989, 1990), Sami and Desrochers (1992) and Brunton and Copper (1994). Descriptions of strata beneath the exposed succession on Anticosti Island are included in INRS-Pétrole (1974). Surface equivalents of pre- and syn-Taconic strata are described in Desrochers (1988), Desrochers and James (1988), and Desrochers et al. (1998).

Vauréal Formation (Ordovician: Rawtheyan)

The Vauréal Formation, as exposed on Anticosti Island, consists of ~275 m of predominantly grey interbedded micrite, calcarenite, and calcareous mudstone of mid- to outer shelf origin. In the subsurface the total thickness of the formation is between 945 and 1027 m (Roliff 1968; INRS-Pétrole 1974). Of this, the upper 552 m contains graptolites of the *Amplexograptus prominens* biozone (Riva 1988). This is considered to be of Rawtheyan age by Koren (1991). Long and Copper (1994) provisionally subdivided surface exposures of the Vauréal Formation into six conformable members, of which only the upper two have been formally defined (Long and Copper 1987*a*).

Lavache member

The Lavache member is the lowest exposed unit on Anticosti Island. It consists of at least 110 m of interbedded, thin-bedded, flat to wavy laminated micrite and fine to very fine calcarenite, repetitive sets of laminated and thin-bedded nodular argillaceous micrite, and minor laminated calcareous mudstone. Coarse to very coarse grainstones are common. Whereas many of the finer beds appear to be laterally continuous, the calcarenites tend to be discontinuous. Many of the fine to very fine calcarenites are burrowed and have sculptured upper surfaces in the form of pits, trails, and burrows extending down from overlying nodular micrite beds. The base of some of these beds is characterized by thin layers of bioclastic sand, commonly containing well-preserved, disarticulated brachiopods. Hummocky cross-stratification is present locally, with hummocks on the scale of 5 to 10 cm, and separations of 5 to 8 m. These hummocks are best seen in the modern tidal flats as the surface becomes flooded. The upper surfaces of some of these typically sharp-based units contain wrinkle marks (Fig. 3B), probably formed by wave-shock-induced fabric collapse (Long 1993*c*, 1997).

Tower member

The Tower member consists of 23 to 35 m of interbedded, graded-laminated micrite and calcareous mudstone with only minor evidence of bioturbation, mostly as surface trails (Figs. 3C, 3D). Rare calcarenite beds reflect intense storm events.

Homard member

The Homard member is a 52 to 72 m thick succession of predominantly thin-bedded subnodular to nodular (bioturbated) micrites and interbedded calcareous mudstones, with prominent calcarenites of very fine and coarse to very coarse sand grade. Calcarenites of very fine sand to small pebble conglomerate grade at first appear to have extensive lateral

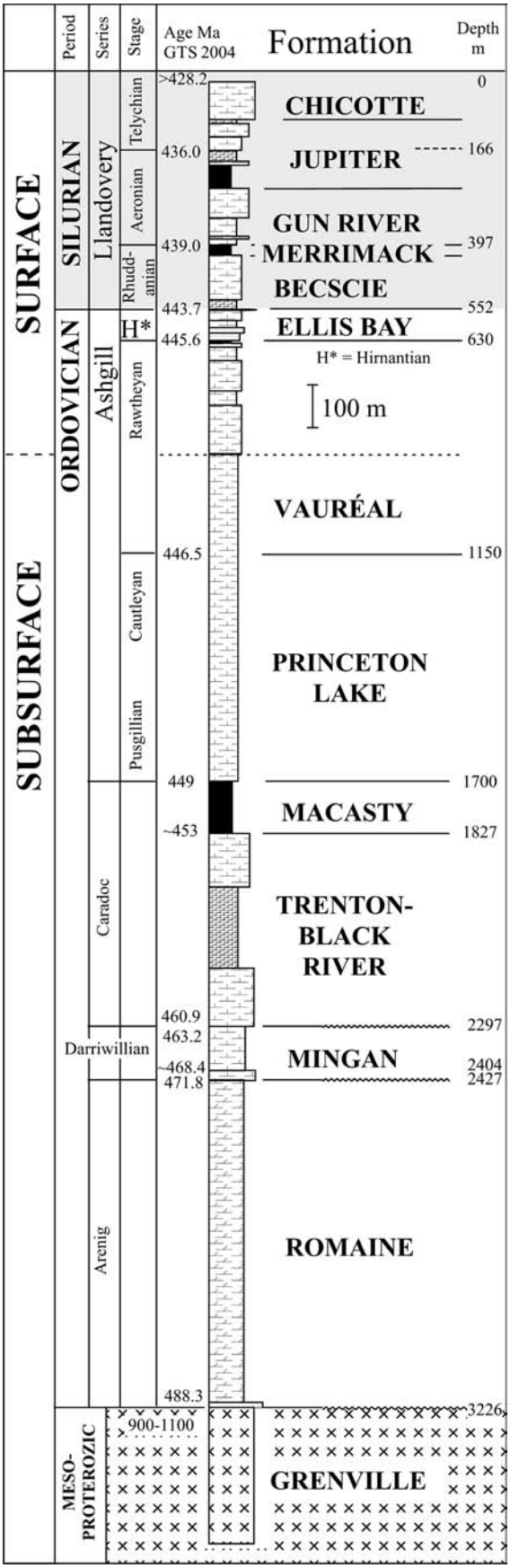

Fig. 2. Surface and subsurface stratigraphy of Anticosti Island, based on boreholes and surface sections from near Jupiter River. Age of stage boundaries from Cooper and Sadler (2004), and Melchin et al. (2004). GTS 2004 = Geological Time Scale 2004.

continuity. In detail, the bases of some of these units are clearly erosional, with large-scale elements including channels up to 1 m deep and at least 12 m wide. Pitted erosional surfaces, and erect hoodoo-like forms, known as "brioche" because of their resemblance to a variety of French bread (Baldwin and Johnston 1977; Long 1997), are developed locally.

Joseph Point member

The Joseph Point member is a 31 to 37 m thick succession of calcareous mudstones, with lesser laminated and nodular micrites and minor calcarenites. In places near the base of the member, micrites are clearly arranged in the form of 8 to 12 m wide channels (up to 1.5 m deep), which appear to be oriented parallel to storm currents as indicated by the orientation of associated aulacerids.

Mill Bay Member

The Mill Bay Member was formally defined by Long and Copper (1987*a*, p. 1810) to include 9.65 m of "resistant weathering, laminated to medium-bedded, commonly cross-bedded, medium- to coarse-grained sandstones, interbedded with laminated carbonate siltstones and minor thin shales" seen in exposures at the east end of Anticosti Island. At the western end of the island, the member is dominated by highly bioturbated, subnodular, thin- to thick-bedded micrites, with minor calcarenites and argillaceous calcilutites. Firmground surfaces developed on micritic to calcarenitic limestones appear to have acted as the foundation for fields of Aulacera, some of which can still be found in growth position.

Schmitt Creek Member

The Schmitt Creek Member consists of 5 to 6 m of recessive weathering, laminated nodular calcareous mudstones and nodular muddy limestones, with minor thin, discontinuous beds of laminated to very thin-bedded lime sandstones and siltstones (Long and Copper 1987*a*).

Ellis Bay Formation (Ordovician: Hirnantian)

The Ellis Bay Formation consists of 52 to 72 m of predominantly grey strata that pass from micritic limestones with abundant sets of calcareous mudstone layers at the west end of the island, to micrites plus mixed carbonate–siliciclastic sandstones at the east end (Long and Copper 1987*b*). The formation marks a period of faunal change from typical Ordovician to Silurian fauna and includes the type section of the Gamachian in North America. An exclusive Hirnantian age for the formation is disputed by some authors, who believe that most of the formation is of latest Rawtheyan age and that only the uppermost one or two members are Hirnantian (Brenchley et al. 1994; Fortey et al. 1995; Underwood et al. 1997). The formation has been formally divided into six members by Long and Copper (1987*a*).

Fig. 3. (A) Tiered bioturbation in micrite from the Macgilvray Member of the Gun River Formation. Note that original soft to firmground burrows (d = 1 cm), with light-coloured diagenetic haloes, were refilled with micrite, which was later invaded by smaller diameter organisms that produced 2–3 mm lined burrows. Upper surface appears to have been blackened, possibly by microbial boring, and residual holes filled with micrite intraclasts during a subsequent storm event. (B) Wrinkle marks on top of hummocky cross-stratified bed in Homard Member, Vauréal Formation, at English Head, west end of Anticosti Island. (C) Zipper-like tracks (*Saerichnites abruptus*) and shallow burrows (*Teichichnus)* on top of hummocky cross-stratified bed, indicating selective harvesting of post-storm mud layer, Vauréal Formation. (D) Shallow surface trails on top of micrite bed in Vauréal Formation. (E) Local overhang, developed by erosion of reefs in the Laframboise Member of the Ellis Bay Formation. Basal part of the Becscie Formation contains highly bioturbated micrites, crinoidal–bioclastic grainstones, and pelletal very fine carbonate sandstones with hummocky cross-stratification, locally distorted into ball-and-pillow structures.

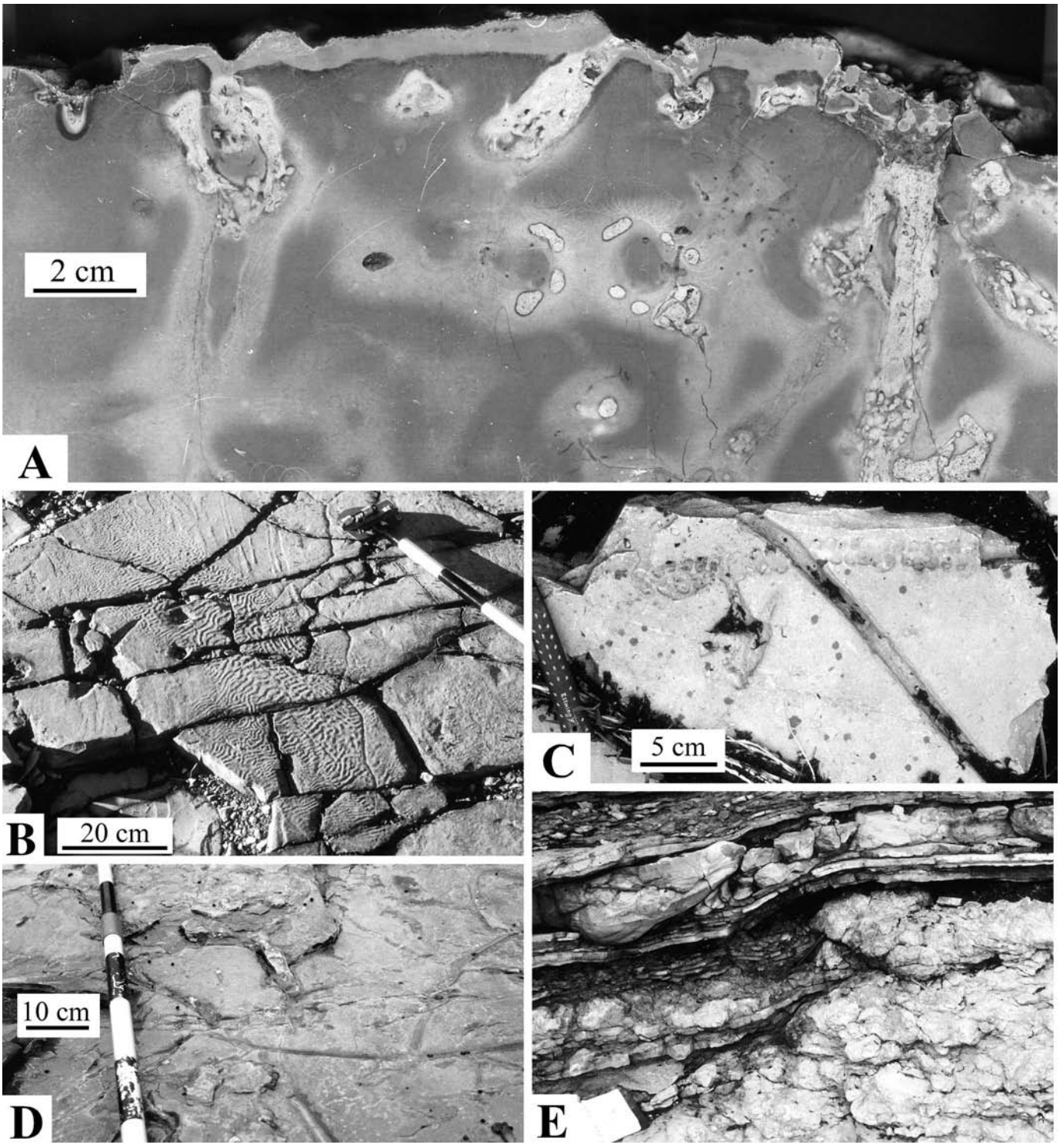

Grindstone Member

The Grindstone Member, at its type section on the northeast coast of Anticosti Island, consists of >14 m of laminated to thin-bedded, very fine sandstones (subfeldspathic to feldspathic bioarenites) and minor laminated calcareous mudstones. These mixed siliciclastic–carbonate sandstones appear to be restricted to the east end of the island; within 15 km of the type section they pass into sandy limestones. To the west, at Vauréal Falls, they are dominated by highly bioturbated thin-bedded micrites, interbedded with thin to thick beds of calcarenite of coarse sand to granule grade. At the west end of the island the member consists of 21 m of predominantly laminated to thin-bedded planar to wavy laminate (irregular, subnodular) micrites, with abundant bioturbation. Grainstones are rare and are typically discontinuous lenticular.

Velleda Member

The Velleda Member in its type section along the northeast coast consists of about 10 m of laminated siltstone and claystone, laminated to thin-bedded, fine and very fine sandstone, with minor coarse sandstone and nodular micrite. In the western sections, the member is 15 m thick and is dominated by interbedded massive to laminated and thin-bedded micrites, calcareous mudstones, and grainstones. Individual micrite beds are typically 3 to 15 cm thick and have a sharp, planar base overlain by a thin layer of broken fossils. This basal lag is overlain by massive to weakly laminated micrite (floatstone), which appears to be partially bioturbated. *Chondrites* burrows are common, commonly forming 2% to 5% of the rock. The upper surfaces of the micrites, and parts of the overlying calcareous mudstones, are pitted and burrowed. The lateral continuity of individual beds is high (tens of metres) although some thinning and thickening are evident along strike. Larger scale architectural elements, including channels and symmetrical, draped waveforms are apparent in the cliff face and in tidal-flat exposures.

Prinsta Member

The Prinsta Member in its type section on the northeast coast consists of 9 m of fossiliferous laminated and nodular calcareous mudstones, with minor thin sandstone and limestone beds. At the west end of Anticosti Island, the member is 17 to 19 m thick and is dominated by highly fossiliferous subnodular to nodular thin-bedded micrites. Minor grainstones and plane to wavy laminated siltstone beds are apparent near the top of the member.

Lousy Cove Member

At its type section along the northeast coast of Anticosti Island the Lousy Cove Member consists of 15 to 16 m of interbedded, laminated, calcareous mudstone and limestone, with minor sandstones. The upper few metres of the member are dominated by flat to wavy laminated micrites, interbedded with calcareous mudstones. These micrites typically have sharp bases, with a thin layer of disarticulated fossils, and a pitted top. At the west end of the island, the member consists of about 18 m of predominantly nodular to subnodular micrite, with about 10% to 15% interbedded calcareous mudstone. The lower 5 m of the member are recessive and may be dominated by mudstones. The upper 3 m of the member are dominated by hummocky and swaley cross-stratified, very fine sand-grade calcarenites.

Laframboise Member

The Laframboise Member is between 0.47 and 8 m thick. In most sections, it begins with an oncolite-rich bed that rests on a burrowed and pitted surface developed on the top of the Lousy Cove Member. This “platform bed” is not the only oncolitic horizon within the member, but is the most persistent and may represent a condensed interval. In most localities, the member is characterized by biohermal masses of coral-, stromatoporoid-, and algal-rich mudstone and wackestone. These are surrounded by inter-reefal strata dominated by highly bioturbated, nodular to subnodular micritic floatstones, in poorly defined beds 5 to 8 cm thick. Locally, calcarenite grainstones, intraformational conglomerates, and oncolitic grainstones are present. The upper surface of the member is irregular, and shows signs of erosion prior to deposition of the Becscie Formation (Fig. 3E). These signs include hardground borers and a locally blackened surface, possibly indicative of intertidal exposure (Long 1997). Carden (1995) found minor high-luminosity spar-cements from reef cavities near the top of the member, indicating at least a brief period of exposure to fresh water.

Becscie Formation (Late Ordovician: Hirnantian to Silurian: Rhuddanian)

The Becscie Formation consists of 124 to 126 m of predominantly light grey to pale yellow micrite and calcarenite that has been divided into two members (Copper and Long 1989; Sami 1989; Sami and Desrochers 1992; Long and Copper 1994).

Fox Point member

The basal Fox Point member is dominated by thin-bedded sets of relatively clean unlaminated and laminated micrite, which are separated by thin sets of siliciclastic-rich carbonate mudstones. The lower part of the unit contains abundant discontinuous grainstone and carbonate sandstone units, with hummocky cross-stratification and local development of ball-and-pillow structures in proximity to stepped irregularities on the basal flooding surface (Fig. 3E; Long and Copper 1994). The Fox Point member thins from 22 m in the west to as little as 3.6 m in the east (Sami 1989).

Chabot member

The overlying Chabot member is characterized by a greater abundance of grainstones and intraformational conglomerates of storm origin.

Merrimack Formation (Silurian: late Rhuddanian)

The Merrimack Formation (Copper and Long 1989) consists of up to 25 m of dark grey, recessive weathering calcareous mudstones, with minor micrites and calcarenites. At the east end of the island the formation contains a few prominent ledges of medium to fine sand-grade calcarenite, characterized by hummocky or swaley cross-stratification. Some of these laterally discontinuous beds have scoured bases. Abrupt lateral termination of some beds may indicate early lithification and partial removal by later storms (Fig. 4A). Associated resistant ledges of apparently massive micrite may also be of storm

Fig. 4. (A) Laterally discontinuous carbonate sandstone with hummocky cross-stratification and scoured margins (cf. Fig. 5E) in Merrimack Formation, northeast coast. (B) Highly bioturbated micrites in Gun River Formation, southwest coast. (C) Micrite-filled channels (1 to 2.5 m above prominent marker bed), upper Macgilvray Member, east end of Anticosti Island.

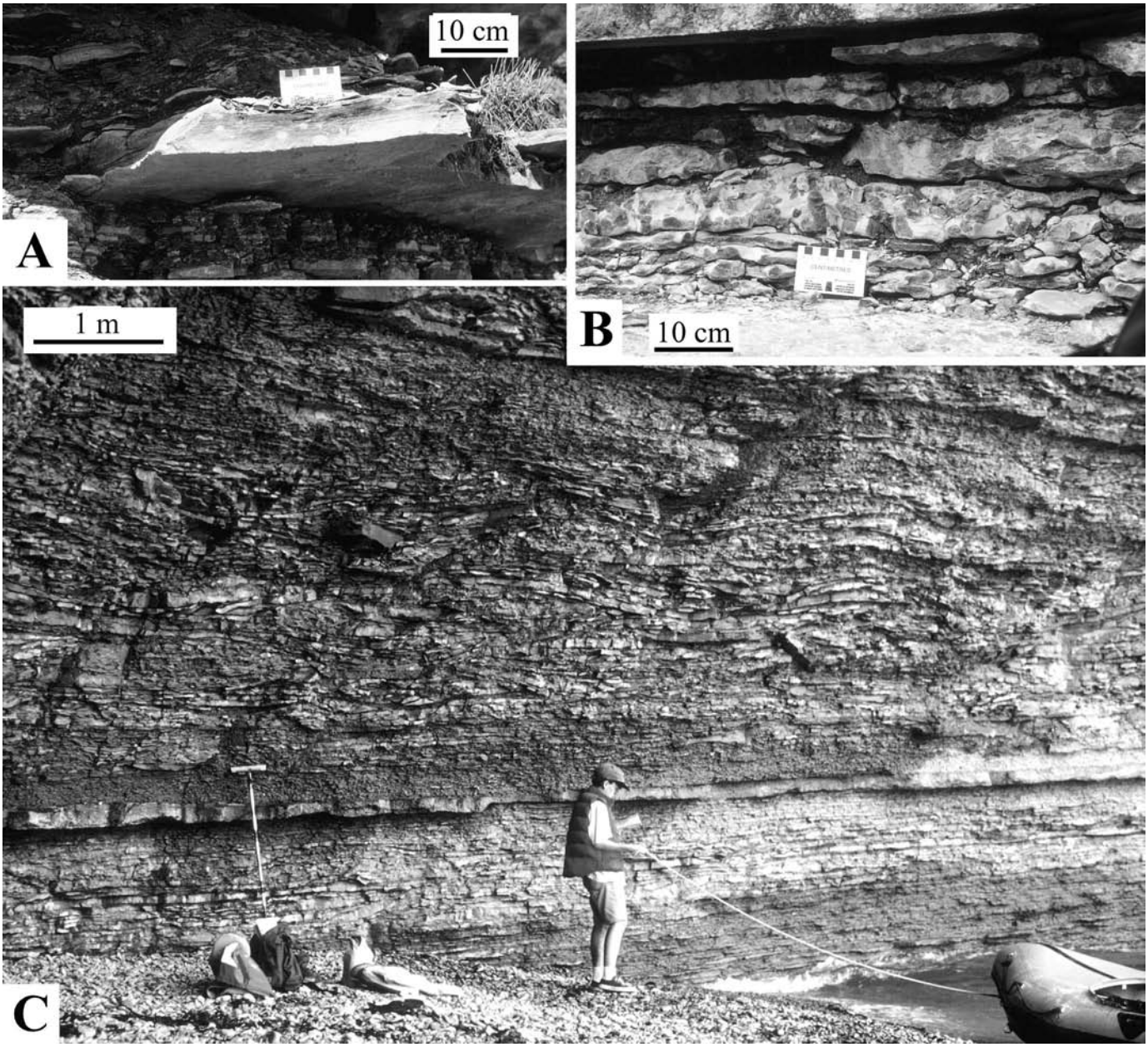

origin. They are characteristically 10 to 12 cm thick and have a sharp flat to wavy base, and a pitted top, with 5% to 10% *Planolites* burrows.

Gun River Formation (Silurian: Aeronian)

Along the northeast coast of Anticosti Island the Gun River Formation includes 85 to 90 m of grey to pale yellow weathering strata, which have been divided into four informal members (Lachute, Innommée, Sandtop, and Macgilvray) that can be traced with some confidence into the type section on the southwest coast (Long and Copper 1994).

Lachute member

The Lachute member consists of 14 to 16 m of resistant weathering, light to medium grey, thinly bedded (2 to 5 cm), irregular to nodular micrites with abundant mudstone partings and minor bioclastic lags. Most of the micrites appear massive, although some exhibit thin planar lamination. The calcareous mudstone partings that form 5% to 10% of the member are usually <2 cm thick and decrease in abundance upsection. The upper 3 m of the member are predominantly weakly bioturbated (bioturbation index, BI = 2: Droser and Bottjer 1989) subnodular micrites, with <5% mudstone partings and minor discontinuous intraformational conglomerate in lenses (? gutter fills) up to 4 cm deep and 40 cm wide.

Innommée member

The conformably overlying Innommée member consists

of 6 to 7 m of strata. At the east end of the island, these include laminated calcareous mudstone and massive to planar cross-stratified calcarenites of very fine to very coarse sand grade. Sections along the south coast are dominated by hummocky cross-stratified carbonates of fine to very fine sand grade, with subordinate micrites and coarse to very coarse sand-grade calcarenites.

Sandtop member

At its type location at the east end of Anticosti Island, the 35 to 40 m thick Sandtop member is dominated by massive to weakly planar to wavy laminated micrites, which occur in sharp-based sets 2 to 10 cm thick, separated by thin sets of calcareous mudstone. Mudstones form 30% to 40% of the succession at the base of the member and are typically <2 cm thick. They decrease in abundance (10% to 20%) and thickness up section. Bioturbation is rare, especially in the lower parts of the member, where it is limited to a few surface trails. In the upper part of the member, bioturbation, including *Planolites* surface trails and pits, becomes more common, as do scour features, interpreted as gutter casts. Calcarenite beds are rare. Local pyritic concentrations are present in the form of nodules developed around some fossils and as a coating on some hardgrounds. The upper limit of the member is taken as the base of the first laterally continuous intraformational conglomerate. Equivalent strata along the south coast and at Jupiter River are up to 42 m thick. These are more intensely bioturbated, and contain more fine to very fine sand-grade calcarenite and intraformational conglomerate. The member is only sparsely fossiliferous, with the lowest diversity of any member in the Gun River Formation.

Macgilvray member

The Macgilvray member is characterized by massive, nodular to subnodular micrites, planar and wavy laminated micrites, calcarenites, abundant intraformational conglomerates, and minor calcareous mudstones. The member is from 23 to 24 m thick in the composite section measured along the northeast coast and is only slightly thicker along the southeast coast. In the northeast coastal sections, there is a progressive increase in the abundance of bioturbation in the micrites and in the abundance of intraformational conglomerates upsection. Mudstones form 9% to 10% of the succession near the base of the member, decreasing to about 5% higher in the section. Thin sets of planar to wavy laminated micrite are replaced upsection by more massive, nodular to subnodular varieties (BI = 1–3). In places, the micrite beds form parts of shallow channels, up to 30 cm deep and 8 m wide (Fig. 4C). The tops and bases of some micrite and hummocky cross-stratified calcarenite units show marked evidence of erosional sculpturing by both storm currents (in the form of gutters) and biological activity (Figs. 3A, 4B, 5A–5D).

Jupiter Formation (Silurian: Aeronian–Telychian)

The Jupiter Formation consists of 164 to 168 m of calcareous mudstone, micrite, grainstone, and minor intraformational conglomerate. Copper and Long (1990) divided the formation into six formal members, named the Goéland, East Point, Richardson, Cybèle, Ferrum, and Pavillon members.

Goéland Member

In the type section, at the east end of the island, the Goéland Member consists of 55 m of recessive weathering, calcareous mudstones and lesser interbedded micritic limestone, and bioclastic grainstone.

East Point Member

At its type locality the East Point Member is about 10 m thick. It consists of a basal calcarenite, overlain by a massive lenticular biohermal unit, and an upper unit of thinly laminated micritic limestone. Inter-reef beds contain minor intraformational conglomerates. Away from the reefs and in areas to the west, the member is characterized by crinoidal grainstones, or coral-rich limestones.

Richardson Member

The Richardson Member consists of 25 m of predominantly argillaceous limestones in the lower part, with resistant layers of micrite and calcarenite occurring in increasing abundance toward the top.

Cybèle Member

The 32 to 34 m thick Cybèle Member is characterized by thin- to medium-bedded, predominantly barren micrites with minor thin calcarenites. Bioturbation and hardground surfaces are common. Laminated calcareous mudstones may be present locally but are poorly exposed.

Ferrum Member

Along the south coast the Ferrum Member is at least 32 m thick. It is characterized by marked lithologic variability with thin-bedded micrite with calcareous mudstone partings, thin calcarenites, hardgrounds, and intraformational conglomerates.

Pavillon Member

The 10 to 12 m thick Pavillon Member consists of recessive calcareous mudstone and interbedded micrite, with discontinuous lenses of calcarenite.

Chicotte Formation (Silurian: late Telychian)

The late Llandovery to ?early Wenlock Chicotte Formation consists of about 90 m of predominantly massive to wavy, thick-bedded, crinoidal grainstone. It contains patch reefs up to 100 m in diameter in at least three horizons, which have been described in detail by Brunton (1988) and Brunton and Copper (1994). Local emergence and karst development are indicated by the presence of rundkarren and solution fissures (Brunton 1988) and abundant irregular truncation surfaces that Desrochers (2004) interprets as erosional disconformities produced at sea-level lowstands. Desrochers (2004) has identified a significant disconformity in the middle part of the formation that could represent a major late Telychian sea-level lowstand.

Sedimentology

Much of the Anticosti succession has been interpreted in terms of deposition by tropical storms, predominantly below fair-weather wave base, in water depths up to 120 m (Long and Copper 1994, 1987*a*, 1987*b*; Sami and Desrochers 1992; Jin et al. 1996; Long 1996, 1997). Tidal-flat deposits are not

Fig. 5. (A) Laterally extensive carbonate sandstones with shallow hummocks (left) and ripples (right), Macgilvray Member, Gun River Formation. HCS, hummocky cross-stratification. (B) Medium to coarse-grained bioclastic sandstone and highly bioturbated micrite, Gun River Formation, southwest coast. (C, D) Discontinuous grainstone units with scoured bases and hummocky cross-stratification, Macgilvray Member, Gun River Formation, southeast coast. (E) Irregular mounds ("brioche") of hummocky cross-stratified calcarenite, buried by highly bioturbated micrites, Gun River Formation. (F) Tempestite bed grading from medium-grained bioclastic sand (1) into pelletal very fine sand with hummocky cross-stratification (2), and capped by highly bioturbated micrite of post-storm origin (3: also present below unit 1), The post-storm unit is capped by two thin sets of flat-laminated micrite (4) representing subsequent smaller scale storm events. Section is in lower metre of Becscie Formation, Laframboise Point, eastern Anticosti Island.

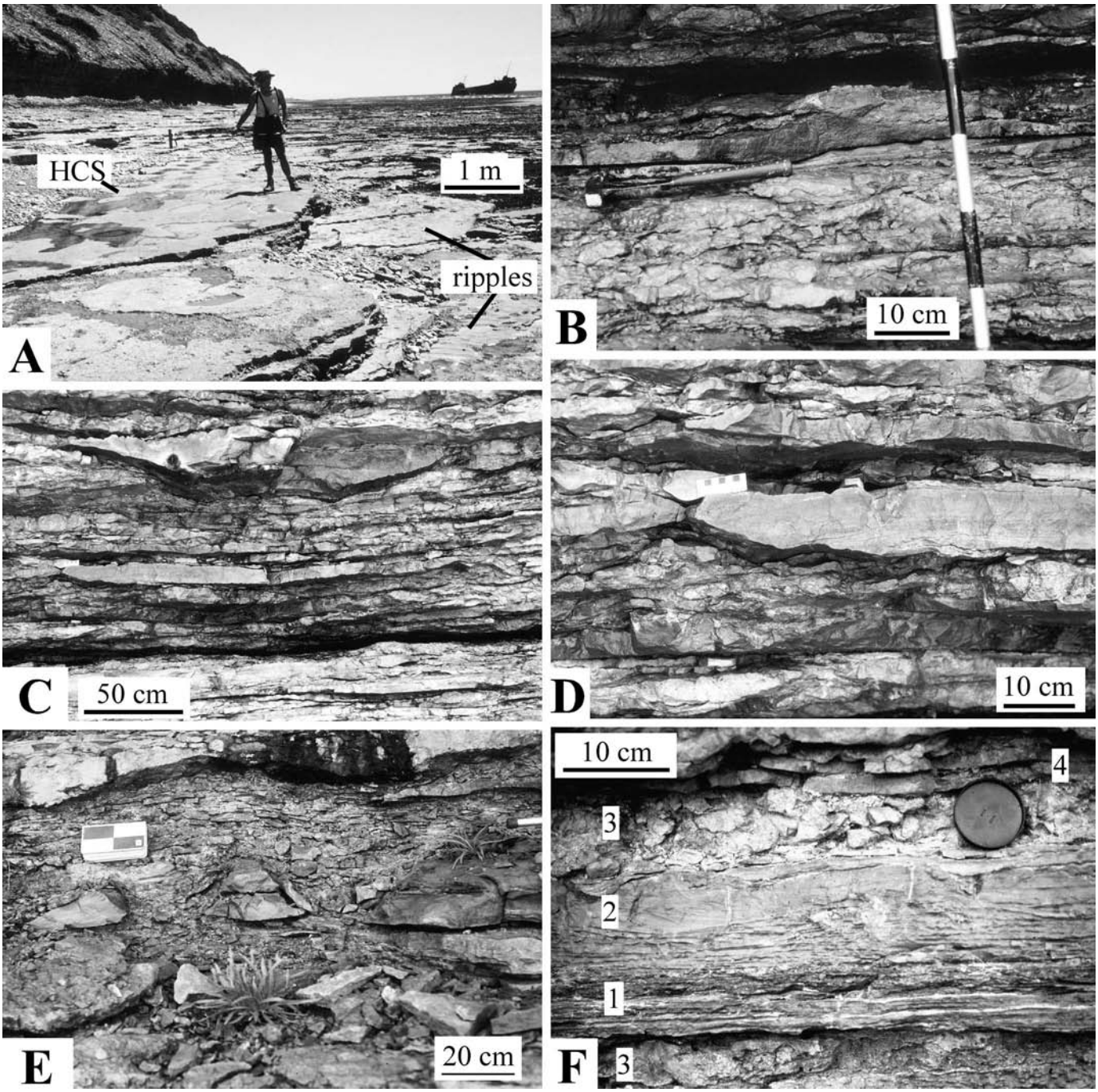

present. Clear evidence of emergence is limited to the Chicotte Formation where a major disconformity has been identified by Desrochers (2004). Possible short-term exposure to fresh water is indicated by the presence of minor high-luminosity spar cements in some of the reef cavities in the Laframboise Member of the Ellis Bay Formation (Carden 1995). In the absence of microkarst features, this may be related to lateral movement of groundwater following shallow burial, rather than direct exposure to rain.

The principal storm indicators (described in the following

subsections) include (1) sharp-based, graded micrites; (2) hummocky cross-stratified sandstones; (3) bioclastic sandstones; and (4) intraclast conglomerates. These tempestites are commonly separated by fair-weather deposits, including massive, laminated, and intensively bioturbated siliciclastic clay-rich carbonate mudstones and marls. Secondary features, indicating storm-induced erosion and sediment remobilization, include gutter casts, pits, "brioche," and ball-and-pillow structures.

Distribution of siliciclastic material, as well as depth-indicative biota and storm indicators, is summarized in Fig. 6. Storm beds (tempestites) all contain minor quantities of quartz and feldspar sand and coarse silt. The sand content refers to the >0.64 mm siliciclastic content of grainstones, hummocky cross-stratified sands, and intraclast conglomerates. Mud content is the siliciclastic clay content of all other beds.

Sharp-based graded micrites

Sharp-based micrites are ubiquitous in all parts of the Anticosti succession, except the Chicotte Formation, which Brunton and Copper (1994) interpret as a storm-influenced, mid-shelf crinoidal shoal and reef complex, and Desrochers (2004) interprets as a near-shore encrinite. Sharp-based graded micrites are best preserved in deeper water strata, where bioturbation is minimal. A typical storm-generated micrite has a high lateral continuity (>50 m), is 2 to 15 cm thick, and has a sharp, erosional base, and a flat to wavy top (Fig. 4C, lower part). Whereas most beds lack visible structures, planar to wavy (?hummocky) lamination is apparent in many beds. Thickness of individual beds may change by as much as 50% along strike lengths of several hundred metres. In places, micrite units are overlain by a 0.2 to 1 cm thick layer of massive calcareous mudstone (marl), but this is normally disrupted by bioturbation.

In more proximal settings, the micrites may have a thin basal layer of broken fossils (including disarticulated brachiopods, tentaculitids, bryozoans, and crinoids) some of which show preferred orientation. Horn corals and gastropods are present locally. This basal lag is overlain by massive to weakly laminated micrite (floatstone), which appears to be partially to wholly bioturbated. *Chondrites* burrows are common, as are *Planolites* and *Phycodes* (Figs. 3C, 3D, 4B, 5B). The upper surfaces of the micrites and parts of the overlying calcareous mudstones are pitted and burrowed (Fig. 3A). Where bioturbation has disrupted more than 60% of the bed, strata typically appear nodular (Figs. 5B, 5F).

Early cementation or microbial, fungal, or algal fixation of some beds is indicated by the local development of firm and hardground surfaces on the top of some micrite beds (Figs. 3A, 7A). Further evidence of early cementation comes from the presence of oval and elongate pits, with locally over-steepened sides (Fig. 7D), analogous to potholes and washouts in modern environments (Hovland 1989). Narrow, straight to sinuous (Figs. 5C, 5D), locally branching forms are interpreted as gutter casts (Aigner 1985).

Hummocky cross-stratified sandstones

Hummocky cross-stratified very fine to fine sandstones are common in the Anticosti succession (Figs. 4A, 5A–5F), both as solitary beds 5 to 25 cm thick and as amalgamated sets 0.5 to >3 m thick. Individual beds appear to have a high lateral continuity and can typically be traced for hundreds of metres in modern tidal flat and cliff exposures, with only minor differences in thickness.

The base of most hummocky cross-stratified beds are sharp, with (in places) a thin, commonly laterally discontinuous basal lag of plane-laminated bioclastic sand or gravel, which may contain abundant fossils, including well-preserved, disarticulated brachiopods. These bioclastic lags are discontinuous and pinch and swell along strike (Figs. 5C, 5D). Lateral continuity is typically highest where the lag is of fine or very fine sand grade, and markedly discontinuous (<5 m) where it is of granule to small pebble grade. The basal lag (where present) is typically gradationally overlain by fine to very fine sandstone with low-angle planar lamination. This grades upwards into hummocky cross-stratification with hummocks on the scale of 5 to 10 cm, and separations of 5 to 12 m (Fig. 5A). In most units, the upper surfaces of beds are planar to subplanar, and commonly lack evidence of well-developed ripple cross-lamination. Most hummocky cross-stratified sand beds are overlain (with sharp contact) by massive or laminated marls, which are commonly intensively bioturbated. In many cases, the upper surfaces of the hummocky units have also been disrupted by intensive bioturbation (Fig. 5F). The upper surfaces of some units are characterized by small ovoid pit-like depressions, 1 to 2 mm deep, 3 to 5 mm wide, and 8 to 15 mm long (Fig. 3B). Similar wrinkle structures (Allen 1984), also referred to as micro-ripples (Fedo and Cooper 1990), kinneyia ripples (Martinsson 1965), and runzelmarken (Reineck 1969), have been interpreted as biogenic in origin by Hagadorn and Bottjer (1997), Noffke et al. (2001), Pruss et al. (2004), and many others. The latter authors suggest that wrinkle marks formed due to collapse following biogenic gas formation beneath a microbial mat. A biological origin for these structures is not likely where they occur within the upper few millimetres of hummocky cross-stratified beds, as it is unlikely that there would be sufficient time for mat development prior to deposition of post-storm mud. A physical origin of these wrinkle structures, involving fabric collapse within a confined porous bed, is more likely (Allen 1982; Kopaska-Merkel and Grannis 1990; Long 1993*c*). It is suggested that initial loose packing of grains in the upper part of the hummocky cross-stratified unit (Cheel 1991; Yagishita et al. 1992) would have made this highly susceptible to fabric collapse soon after deposition due to wave-induced cyclic loading, especially if the bed were confined by a thin layer of post-storm mud. Cyclic application of stress by progressive waves results in a progressive increase in pore pressure (Seed and Rhaman 1978), which would reduce internal shear stress, promote fabric collapse, and result in wrinkle formation. Further wave shock may be responsible for the formation of laterally extensive zones in which the hummocky cross-stratified units have become separated into ball-and-pillow structures over strike lengths of 25 to 250 m (Fig. 3E). The discontinuous nature of these beds excludes a seismic origin.

The upper surface of some pillowed horizons in the Homard member of the Vauréal Formation may have evolved into a firm or hardground within a few years of pillow development. The upper surface is burrowed and in places acted as a foundation for the growth of crinoids and corals. Further evi-

Fig. 6. Relative abundance of siliciclastics, biological components, and specific bed types in the Anticosti succession. Inferred local water depth (range) indicated on right (after Long 1997). HCS, hummocky cross-stratification.

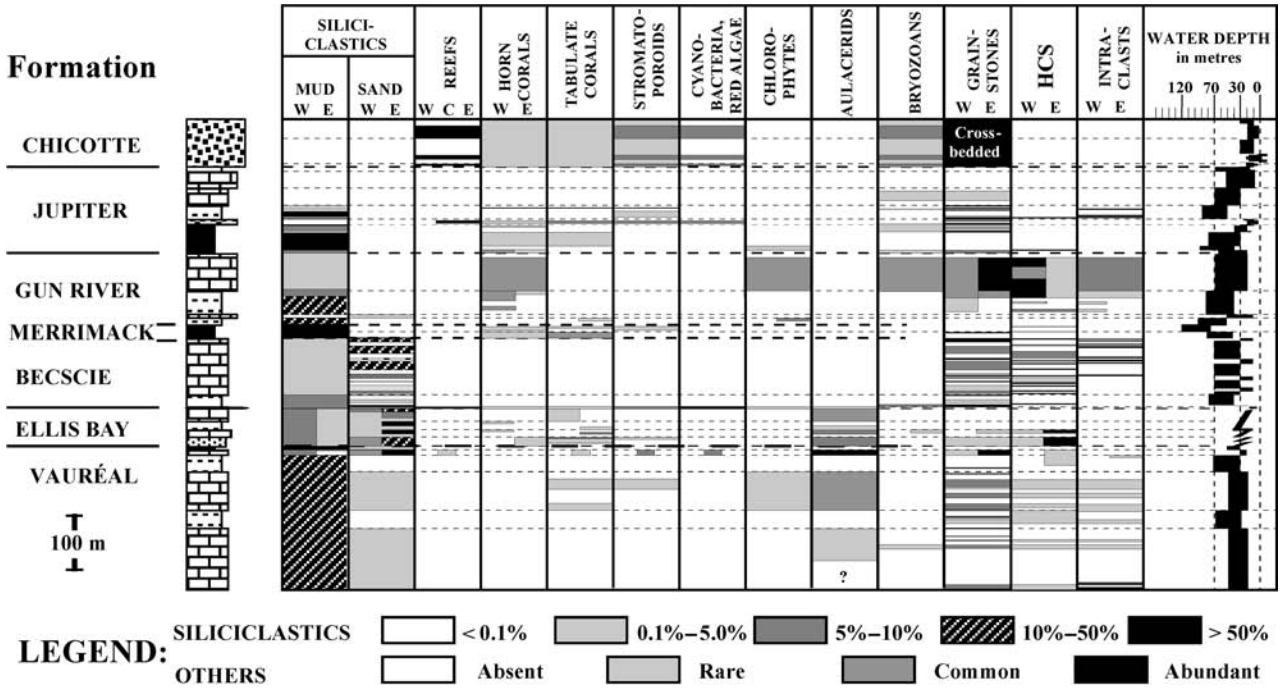

dence for early sea-floor cementation of hummocky cross-stratified units is provided by the sculptured upper surfaces of some beds. This includes abrupt lateral termination of some beds in the Merrimack Formation (Fig. 4A) and development of sculptured erosional bedforms (including "brioche") in the Vauréal and Gun River Formations (Fig. 4E).

Bioclastic sandstones

Bioclastic grainstones of medium sand to granule grade are common in all parts of the Anticosti succession, except the Merrimack Formation, and are the principal lithotype in the Chicotte Formation (Fig. 6). They occur both as discontinuous basal lags at the base of some sharp-based graded micrites and hummocky cross-stratified fine to very fine sandstone (Fig. 5F), and as discrete beds from 2 mm to 50 cm thick. The latter are either graded, massive, or plane-laminated and lenticular over tens of metres, or occur as (rare) massive or planar to trough cross-stratified, discontinuous lenticular sets (Figs. 5B–5D). Most units have sharp, planar erosional lower contacts, although irregular basal contacts are common where the sand has infilled burrows in underlying firm- or hardground surfaces (tubular tempestites of Wanless et al. 1988).

Laterally continuous sets are most commonly found in parts of the succession where graded micrites contain only minor evidence of bioturbation. Where highly bioturbated (>50%) micrites are present, they are scarce to absent. Amalgamated sets of ripple and dune cross-stratified grainstones are common only in the Chicotte Formation, and locally in the Vauréal, Ellis Bay, and Gun River formations. Channellized, siliciclastic-rich grainstones (with sandstone intraclasts and reworked, overturned corals) are restricted to the upper part of sand-wave complexes in the Grindstone Member of the Ellis Bay Formation at the east end of Anticosti Island (Long and Copper 1987*a*, 1987*b*).

Intraclast conglomerates

Flat-pebble, intraclast conglomerates are common in the Silurian Becscie, Gun River, and Jupiter formations and rare in the Ordovician Vauréal Formation. They typically occur as even parallel beds, which can be traced laterally for tens to hundreds of metres. The lower contacts are typically sharp, planar to stepped erosional surfaces, except where they locally infill burrows and pits in underlying hard- or firmground surfaces (Figs. 3A, 7A). The conglomerates typically have a locally imbricated contact framework with 30% to 70% rounded, platy to discoid pebbles, in places supported by a matrix of bioclastic medium to very coarse sand or granule conglomerate. The flat pebbles consist almost entirely of locally derived micrite. These may have been derived from the upper few centimetres of the sea floor by selective scouring of burrows, and subsequent undercutting and reworking of the early lithified crusts during storms. Some clasts have a "Swiss cheese" appearance, in which some of the enlarged burrow entrances are preserved (Figs. 7B, 7C).

Storm patterns and siliciclastic distribution

Typical models of proximality trends in carbonate tempestites suggest that graded bioclastic sandstones and intraclasts are most abundant in shallower, inshore settings and are replaced offshore by hummocky cross-stratified sands, then in progressively deeper water by sharp-based graded micrites and finally marls (Aigner 1985). In the Anticosti succession, whereas lenticular and cross-stratified grainstones may have been more abundant in shallower water settings

Fig. 7. (A) Stepped erosional surface at base of intraclast rudstone, Macgilvray Member, Gun River Formation. Note blackening of bed and clast contacts (1), as well as firm-ground (3) and minor hardground borings (*Trypanites*, 2). (B, C) Platy, in part perforated, intraclasts in intraclast rudstones of the Macgilvray Member, Gun River Formation. (D) Oval pit formed by partial removal of semi-consolidated surface, Tower Member, Vauréal Formation.

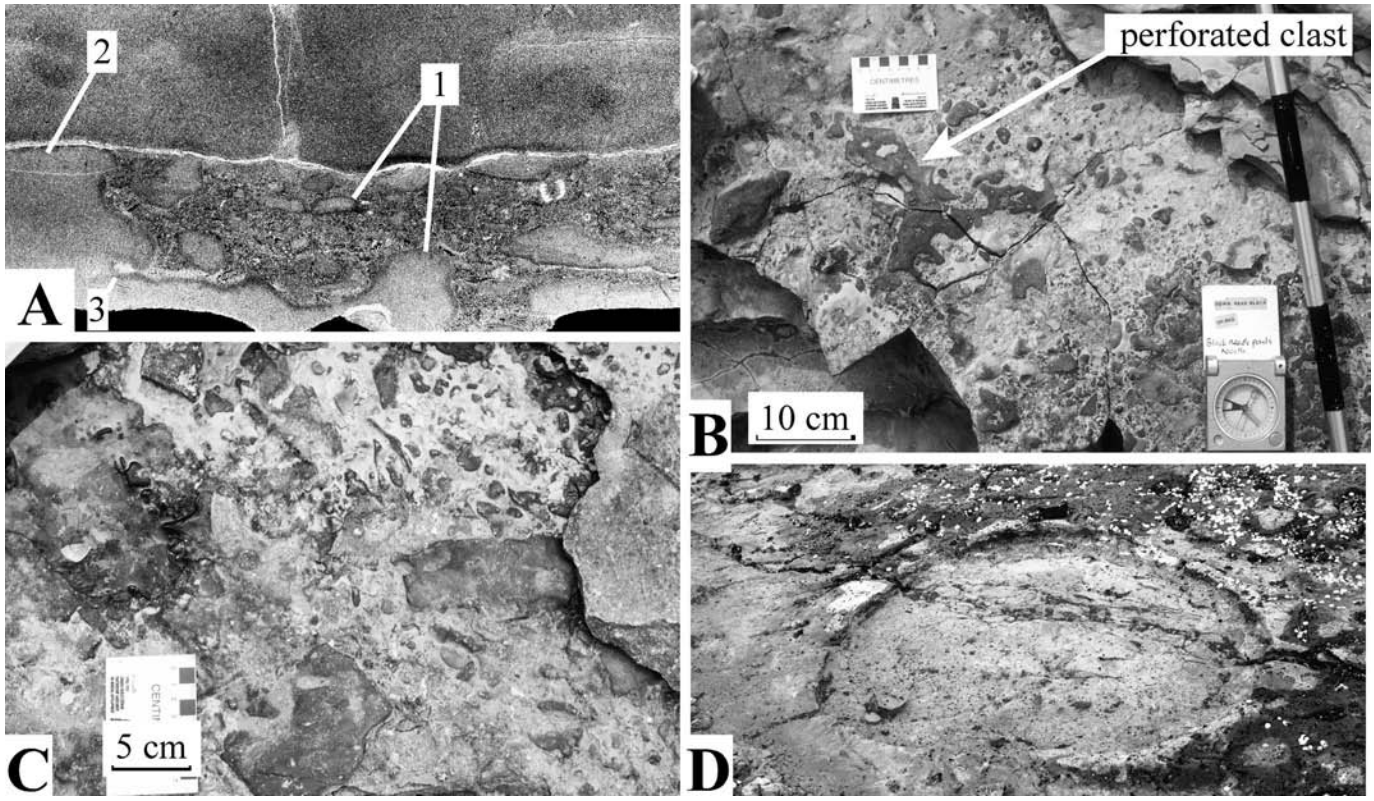

near to or above fair-weather wave base, the greatest abundance of intraclast conglomerates and laterally continuous graded and laminated bioclastic grainstones may have been seaward of the hummocky cross-stratified zone (Sami and Desrochers 1992). Abundance of intraclasts may be related to both storm frequency and the rate of early sea-floor lithification. Sepkoski (1982) notes that flat-pebble conglomerates are rare after the Cambrian, possibly due to the expansion of infauna. Abundance of flat-pebble conglomerates in the Anticosti succession, especially in the Silurian, may indicate a reduction in the abundance of vertical bioturbators, or restriction of their depth range following the Ordovician–Silurian extinction event (cf. Pruss et al. 2005).

The minimum frequency of major storm events can be assessed in parts of the succession using density bands on corals. For example, strata of mid-shelf origin in the Vauréal Formation contain the coral *Paleofavosites* with 7 to 15 annulations suggesting a minimal large-storm interval of 7 years.

The presence of abundant feldspar, strained quartz, metamorphic and igneous rock fragments in sandstones from the Ellis Bay Formation suggests that the most likely source for siliciclastic material was the late Precambrian Grenville Province, now exposed 30 to 40 km north of Anticosti Island, along the north shore of the St. Lawrence River (Long and Copper 1987*b*). This may have been transported into the basin by southwesterly directed longshore drift, from point sources along the west side of the Strait of Belle Isle, and spread across the shelf by storm-induced geostrophic currents.

As gutter casts and elongate fossils tend to line up with storm-induced geostrophic current systems in mid- and outer shelf settings, their net orientation can be used to evaluate changes in shoreline geometry (Aigner 1985; Duke 1985; Long and Copper 1987*b*). During deposition of the Vauréal Formation, geostrophic currents appear to have been parallel to the west coast of the Strait of Belle Isle. This NNW–SSE trend shifted progressively clockwise by 120° during the Llandovery (Long 1997). The change in inferred shoreline geometry may reflect changes in geometry related to flooding of the shield, infill of the foreland basin between Newfoundland and the mainland, or partial uplift at the north end of the Strait of Belle Isle due to marked reduction of tectonic loading. Absence of a marked siliciclastic component in the Chicotte Formation may reflect a northward shift in coastlines, combined with development of coastal boundary currents. Rising Taconic highlands in the Gaspé region (Malo 2004) do not appear to have contributed significantly to the sediment supply on the Anticosti Platform, as the siliciclastic component does not include recycled sedimentary or volcanic lithic material.

Tectonic setting and subsidence history

The Anticosti Platform originally developed as a passive-

Fig. 8. Subsidence history of Anticosti by back-stripping analysis, using Subside! for Macintosh by M.S.Wilkerson and Associates (undated). P-C, Pushgillian–Coutleyan; Rhu, Rhuddanian; Aer, Aeronian; Tely, Telychian.

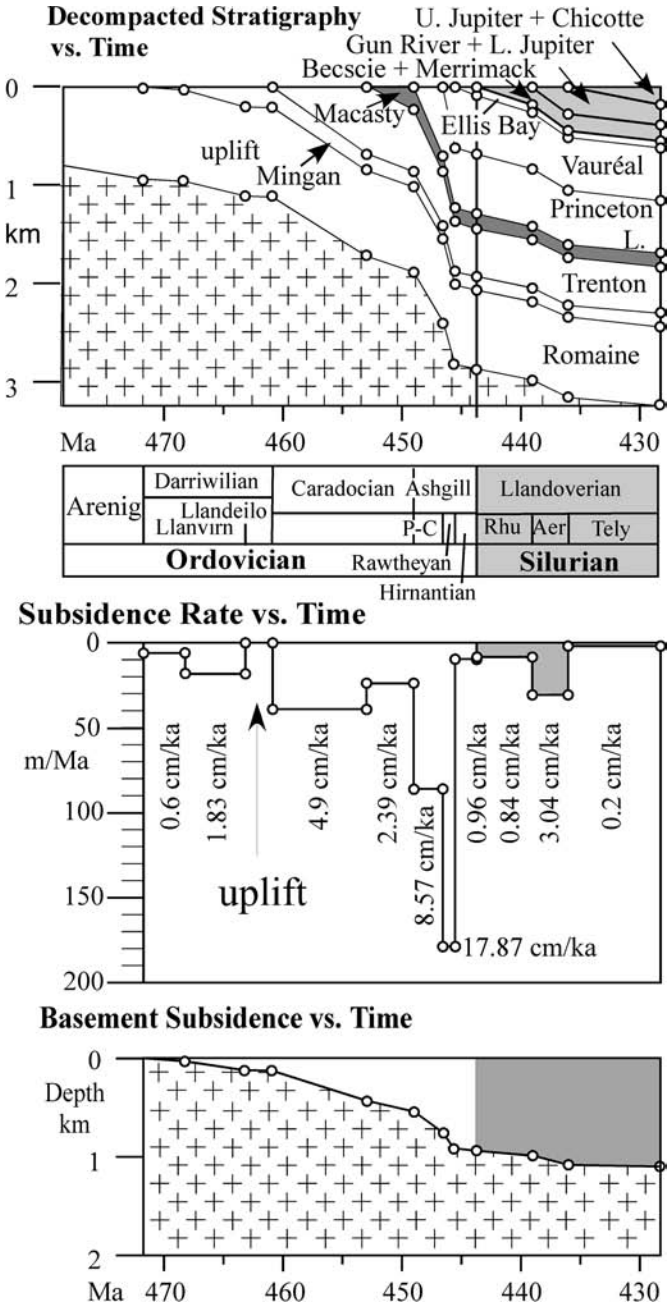

margin succession along a transform segment of the Laurentian continental margin, generated by the opening of the Iapetus Ocean in late Neoproterozoic times (Waldron et al. 1998; Cousineau and Longuépée 2003; Malo 2004). The St. Lawrence Promontory appears to have developed as an upper-plate segment of an irregular continental margin, as it does not contain a significant cover of early Cambrian strata (Roliff 1968; Waldron et al. 1998; Lavoie et al. 2003).

The subsidence history of the Anticosti basin was evaluated using back-stripping models (Fig. 8; see Allen and Allen 1990 for methodology). In this study, stratal units shown in Fig. 2 were decompacted, and the effect of progressive sediment loading removed from overall subsidence to calculate net tectonic subsidence, using Wilkerson and Associates' "Subside!" program for Macintosh computers. Thermal subsidence in the basin during deposition of the Romaine Formation is estimated at about 0.6 cm/ka (Fig. 8, middle part). The passive margin was later transformed into a foreland basin by closure of the Iapetus Ocean. Differential subsidence within the basin can be related to asymmetric obductive loading of the Laurentian plate margin by thrust sheets from within rising highlands in both the Gaspé and Miramichi areas to the southwest, and in the Humber terrane to the east (Long and Copper 1987*b*; Stockmal et al. 1995; Waldron et al. 1998; Cousineau and Longuépée 2003; Lavoie et al. 2003; Malo 2004), combined with sediment-induced loading (Long 1993*a*). Initial thrust loading along the Newfoundland margin, beginning in the late Arenig (Waldron et al. 1998), resulted in migration of a foreland bulge onto the craton. This produced a marked unconformity at the top of the Romaine Formation (Desrochers 1988; Desrochers and James 1988; Desrochers et al. 1998).

Malo (2004) indicated that the first nappes to override the St. Lawrence transform fault, south of Anticosti Island, did so between 459 and 456 Ma. This, and subsequent thrust loading, appear to have had a direct influence on sediment facies within the Trenton–Black River units, with net thermal subsidence and tectonic loading increasing from 1.8 cm/ka during deposition of the Mingan Formation to 4.9 cm/ka during deposition of the Trenton–Black River strata (Fig. 8). The presence of emerging tectonic highlands in the Gaspé also directly influenced the morphodynamics of the St. Lawrence Platform, by blocking storms tracking from the southeast. During lowstands the foreland basin may have been closed to the west to form a marine embayment. At highstands, a greater part of the craton was flooded and an open seaway may have developed between the Anticosti basin and the continental interior (Long and Copper 1987*b*).

Continued subsidence during the late Caradocian, combined with rapid sea-level rise led to deposition of organic-rich mudstones (Macasty Formation) within the sediment-tarved Anticosti basin (Malo 2004). Estimated subsidence on the margin at this stage fell to about 2.4 cm/ka (Fig. 8). Renewed thrusting from the south in the Ashgill, combined with residual thermal subsidence, led to a marked increase in basement subsidence to 8.6 cm/ka during deposition of the Princeton Lake Formation, reaching a peak of 17.9 cm/ka during deposition of the Vauréal Formation (Fig. 8; Table 1). This may have been driven by sinistral shear at this time between North Africa and Laurentia (Stockmal et al. 1995).

Thrust loading from the south appears to have halted in the Hirnantian, with basement subsidence slowing to <1 cm/ka during deposition of the Ellis Bay Formation, and 0.8 cm/ka during deposition of the Becscie and Merrimack formations (Fig. 8; Table 1). An increase to 3.0 cm/ka in the Aeronian may indicate a minor renewal of thrusting from the Gaspé during deposition of the Gun River Formation and the lower part of the Jupiter Formation. Subsidence in the Telychian, during deposition of the upper part of the Jupiter Formation and overlying encrinites of the Chicotte Formation, appears to be as low as 0.2 cm/ka. This may be an underestimate as the depositional record of the Chicotte Formation

Table 1. Expected thickness of tempestite cycles if driven by cosmic (Milankovitch style) cyclicity (duration of Ordovician–Silurian stages after Cooper and Sadler 2004 and Melchin et al. 2004; duration of cycles after Berger and Loutre 1994).

Stage	Thickness (m)	Time (ka)	Eccentricity		Obliquity		Precession		Tectonic subsidence
			m/400 ka	m/100 ka	m/30 546 a	m/37 222 a	m/16 399 a	m/19 297 a	cm/ka
Telychian	166	7800	8.51	2.13	0.65	0.79	0.35	0.41	0.20
Aeronian	231	3000	30.80	7.70	2.35	2.87	1.26	1.49	3.04
Rhuddanian	155	4700	13.19	3.30	1.01	1.23	0.54	0.64	0.84
Hirnantian	78	1900	16.42	4.11	1.25	1.53	0.67	0.79	0.96
Rawtheyan	520	900	231.11	57.78	17.65	21.51	9.44	11.15	17.87
Pusgillian + Cautleyan	550	2500	88.00	22.00	6.72	8.19	3.59	4.25	8.57

Note: The tectonic plus thermal induced subsidence rate is based on back-stripping analysis in Fig. 8.

may be incomplete due to the development of a marked disconformity about 30 m above the base of the formation, because of a rapid fall in global sea level, and the upper age limit of the formation is uncertain.

Eustatic sea levels

In foreland basins, it is not always easy to separate the effects of subsidence from eustatic sea-level change or changes in sediment flux. Sami (1989), Sami and Desrochers (1992), Easthouse and Driese (1988), and Baarli (1988, 1998) suggest that sensitive proxy sea-level curves can be obtained from tempestite frequency analysis, using models pioneered by Aigner and Reineck (1982) and Aigner (1985). These models suggest that tempestites on open shelves should be restricted to water depths greater than fair-weather wave base (about 10–15 m, Swift et al. 1983) and should be thin, fine, and decrease in abundance in progressively deeper water. Campbell (in Dott and Bourgeois 1982) suggests that siliciclastic hummocks could be formed in water depths up to 80 m. The low-relief hummocks developed in many of the fine-grained carbonates in the Anticosti succession could have developed in deeper water, as the peak spacing (6–12 m) indicates long-period waves (cf. Myrow and Southard 1991, 1996). A basic premise of tempestite frequency models is that any upsection increase in shore-proximal facies should indicate decreasing water depth, although a similar trend might also be expected if the intensity of storms increased in response to shifts in climatic belts.

Using bed-by-bed stratigraphic information for the Becscie Formation in Sami (1989) and my observations for the Vauréal, Ellis Bay, Gun River, and lower Jupiter Formations from the Jupiter River area of central Anticosti Island it is possible to generate synthetic sea-level curves which show evidence of 3rd-, 4th-, and 5th- (or higher) order sea-level changes (Read 1995) for slightly over a kilometre of section. Figure 9 shows three possible proxy curves based on (A) frequency of storm beds of silt to gravel grade per metre, (B) relative abundance of storm beds as percentage of preserved section, and (C) weighted abundance of storm beds. The latter curve is generated by multiplying bed thickness by a grain-size-dependent weighting factor (coarse silt = ×1; very fine sand = ×2; fine sand = ×3; and so on). Bioturbation was not taken into consideration in the proximality analysis, as this has not been systematically recorded for the Becscie Formation.

Given that the probable duration of Late Ordovician and Early Silurian stages are reasonably well established (Cooper and Sadler 2004; Melchin et al. 2004), and the thickness of stratigraphic intervals is well defined, it is possible to estimate peak spacings that would coincide with principal astronomical (Milankovitch-style) cycles (Table 1). The most important orbital cycles affecting Recent climate (and therefore storm intensity) are the 100 ka short-period and 400 ka long-period eccentricity cycles, the 54 ka and 41 ka obliquity cycles, and the 23 ka and 19 ka precessional cycles (De Boer and Smith 1994; Read 1995). As the Earth–Moon system was closer together in the Late Ordovician and Early Silurian the obliquity and precessional cycles should be shorter, and have been calculated at 30.5 and 37.2 ka, and 16.4, and 19.3 ka, respectively, by Berger and Loutre (1994).

Fig. 9. Tempestite frequency analysis for Late Ordovician and Early Silurian strata of Anticosti Island. (A) Tempestite beds of silt grade and coarser per metre. (B) Relative abundance of non-micritic tempestite beds per metre. (C) Weighted abundance of tempestite beds. (D) Paleodepth (deeper to left) based on fossil communities (after Long 1996, and Desrochers et al. 1998). (E) Water depth based on conodont community analysis (Zhang and Barnes 2002). (F) Range of possible water depths, based on groups of sedimentary structures (after Long 1997). (G, H) Inferred 4th- and 3rd-order sea-level curves based on smoothing of the weighted tempestite frequency curve (rise to left, fall to right). Stars indicate peaks which may coincide with predicted 100 ka cycles in the Rawtheyan (lower R1 to R7) and Hirnantian (H1 to H4), and 400 ka eccentricity cycles in the Rhuddanian (upper R1 to R13) and Aeronian (A1 to A8). Note that during the Rhuddanian none of the observed peaks coincided with predicted cycle intervals for R2, R3, R5, R7, R9 or R11. Fm., Formation; Mbr., member.

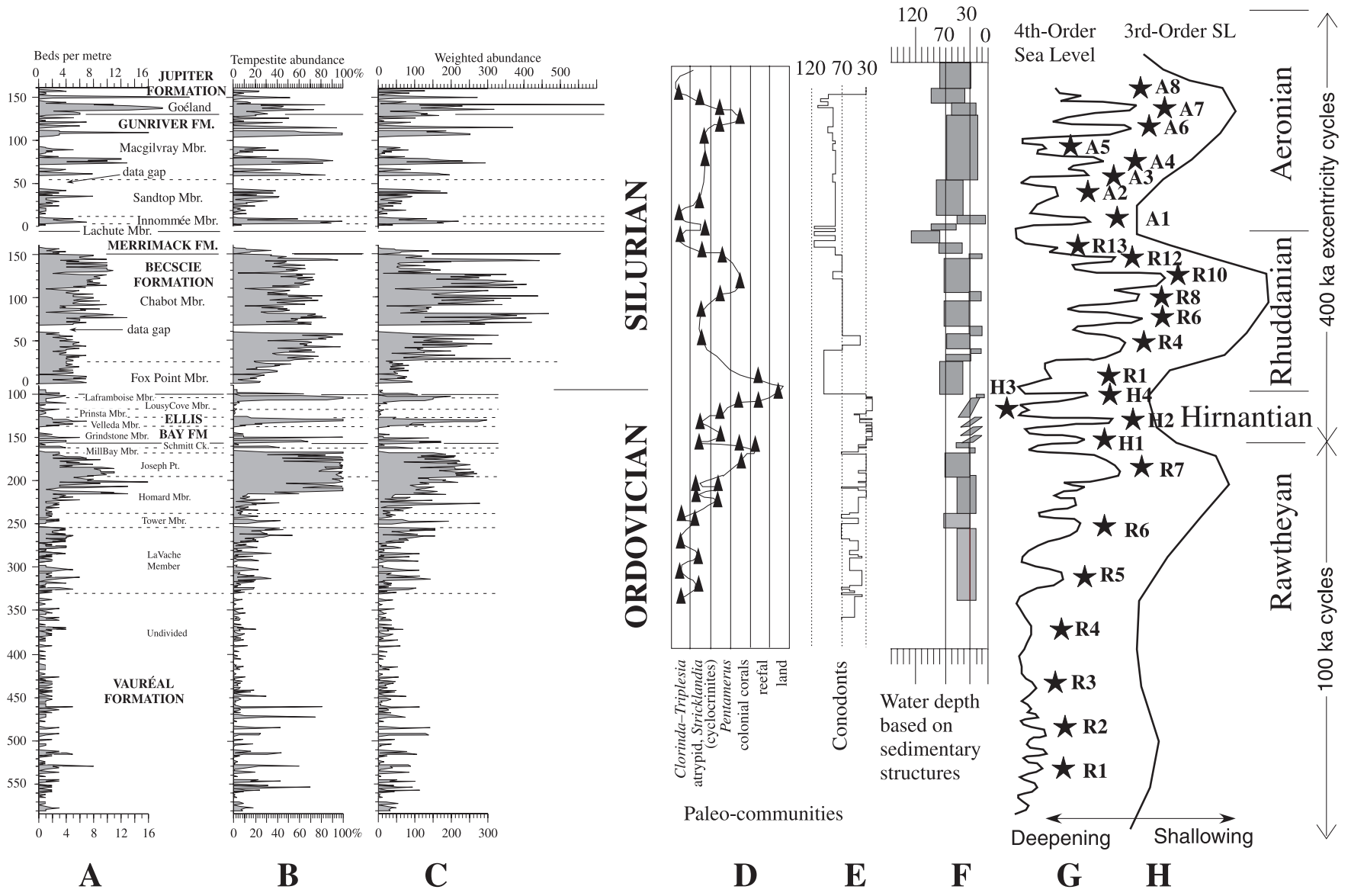

Where the upper and lower age limits of stratigraphic units are known, it is possible to calculate the expected (compacted) thickness of strata corresponding to eccentricity, obliquity, and precessional cycles (Table 1). Comparison of this information with tempestite frequency curves indicates that many of the observed peaks (Figs. 9A, 9B, 9C), correspond closely to predicted 100 ka short-period or 400 ka long-period eccentricity cycles (Fig. 9G), but do not correspond directly to sea-level curves generated using paleo-communities, conodont assemblages, or sedimentary structures (Figs. 9D, 9E, 9F). This may in part be related to the ways in which such curves are generated. The paleo-community curve (Fig. 9D) based on Long (1996) and Desrochers et al. (1998) is based largely on earlier work on fossil communities, in which indicator species were identified in grouped intervals through out the succession. This follows the tradition of using Benthic Assemblages (BA 1 to BA 5) to define shore parallel belts deposited in specific relative water depths (Brett et al. 1993). A problem with this approach is that is assumes that indicator species do not change their ecological habitat with time. The scheme may work well in the Middle to Late Silurian (Brett et al. 1993), but does not work effectively in the Late Ordovician or Early Silurian. For example, both *Eocelia* and *Pentamerus* appear to migrate from deeper water settings in the Lower Jupiter to more typical shallow-water settings (BA 2 and BA 3) in the Telychian. *Eocoelia* (BA 2) and *Clorinda* (BA 5) co-occur in the Richardson Member; and *Eocoelia* (BA 2), *Stricklandia* (BA 4), and *Pentamerus* (BA 3) co-occur in the Ferrum Member. Figure 9E gives an alternate approximate estimate of water depth based on conodont community analysis (Zhang and Barnes 2002), which had been calibrated using depth estimates based on assemblages of sedimentary structures in Long (1997). The latter (Fig. 9F) gives a potential range of water depths for grouped data (based on Fig. 6) and reflects depositional depth and not absolute sea level.

Figures 9G and 9H are progressively smoothed versions of data in Fig. 9C and represent potential 3rd- and 4th-order changes in eustatic sea level plotted against stratigraphic thickness. From the tempestite curves and inferred 4th-order cycles (Figs. 9C, 9G) it appears that Read's (1995) contention that short- and long-term eccentricity cycles should be the dominant signal in glacial periods is justified. In the measured interval through the Vauréal Formation, up to seven short-period (100 ka) eccentricity cycles should be present, with a common spacing of about 38 m. Peaks in the tempestite frequency curves (Fig. 9, columns A to C) support this contention. An upsection increase in peak intensity is probably related to overall shoaling or a slight decrease in net tectonic subsidence rates towards the end of the Rawtheyan (Fig. 9, stars R1 to R7 in column F). Other, shorter period (higher order) peaks are apparent in the lower 200 m of the interval examined. These may reflect shorter period obliquity cycles (18 to 22 m), but cannot be resolved with confidence.

Only three main peaks are seen in the Hirnantian Ellis Bay Formation (H1, H2, and H4). This interval has a predicted duration of 1.9 Ma using the revised isotopic dates in Cooper and Sadler (2004). If short-period eccentricity cycles were dominant in controlling ice volume at the poles, as suggested by Long (1993*a*) and Sutcliffe et al. (2000), at least 19 peaks should be expected (Fig. 10). The apparent deficiency is even more pronounced if only the upper one or two members of the Ellis Bay are Hirnantian in age (cf. Brenchley et al. 1994; Underwood et al. 1997). If cyclicity were controlled by long-period (400 ka) eccentricity, at least four peaks should be recognizable. The presence of a small peak in the Lousy Cove Member might represent the missing peak (H3), or strata may be missing from the succession at the base (burrowed hardground) or top (blackened and bored surface) of the Laframboise Member (slightly below the official Ordovician–Silurian boundary). This represents the shallowest interval in the Anticosti succession prior to a short interval of emergence in the Chicotte Formation (Desrochers 2004).

Major peaks within the Rhuddanian and Aeronian stages appear to be directly controlled (or obscured) by long-period cyclicity (Fig. 9, column F; Fig. 10). Thirteen long-period (13 m) cycles should be present in the Rhuddanian. Matching of frequency curves with the predicted cycle intervals indicates that some cycles (R2, R3, R5, R7, R9, and R11) are missing or have been subdued by higher (smaller scale) cyclicity. All eight (31 m) predicted long-period eccentricity cycles in the Aeronian interval can be matched with confidence (Fig. 9). Once again the peaks in the tempestite frequency curves do not exactly match the sea-level curves predicted earlier using macrofossils or conodonts. Higher order (shorter) cycles may be present, but cannot be resolved with confidence using a 1 m sample interval.

Despite the absence of some predicted peaks, there is a clear indication that both short- and long-term eccentricity cycles directly influenced the deposition of tempestites within the Anticosti succession. These could have been driven by eustatic sea-level change, climatic-induced differences in sediment supply (flux) from shallow-water carbonate factories, or orbital-induced shifts in intensity and position of storm belts. Comparative sea-level curves based on paleontological depth analysis (fig. 9D from Long 1997; Desrochers et al. 1998; Zhang and Barnes 2002) and depth analysis of sedimentary structures (fig. 9E from Long 1997) show roughly similar (3rd-order) trends to those indicated by tempestite frequency analysis, although the brachiopod-based paleodepth curves appear to depart significantly from the tempestite, conodont, and sedimentary structure-based curves in the early Rhuddanian. The tempestite frequency curves appear to have a higher resolution than synthetic sea-level curves generated using cumulative aggregation plots (Diecchio 1995), although long-period events appear to be similar. Most of the high-frequency shoaling events recorded in the Ellis Bay Formation by Long and Copper (1987*b*) and Long (1993*a*, 1993*b*) can be seen in the tempestite curves.

Conclusions

During deposition of the Anticosti succession, the Anticosti basin lay from 10° to 17° south of the equator and was swept by a non-monsoonal, south tropical current (Wilde 1991). For at least seven million years, the basin would have been subject to severe tropical cyclones (hurricanes) during the warm season (Duke 1985), which would explain the abundance of storm-related strata in the Anticosti succession. During the early phase of foreland basin evolution siliciclastic material from estuarine or deltaic sources was

Fig. 10. Comparison of weighted tempestite frequency data (from Fig. 9) with predicted eustatic sea-level curves from the Silurian (top) and Ordovician (bottom) plotted against time (from Cooper and Sadler 2004, and Melchin et al. 2004). Stars indicate dominant cycles from Fig. 9.

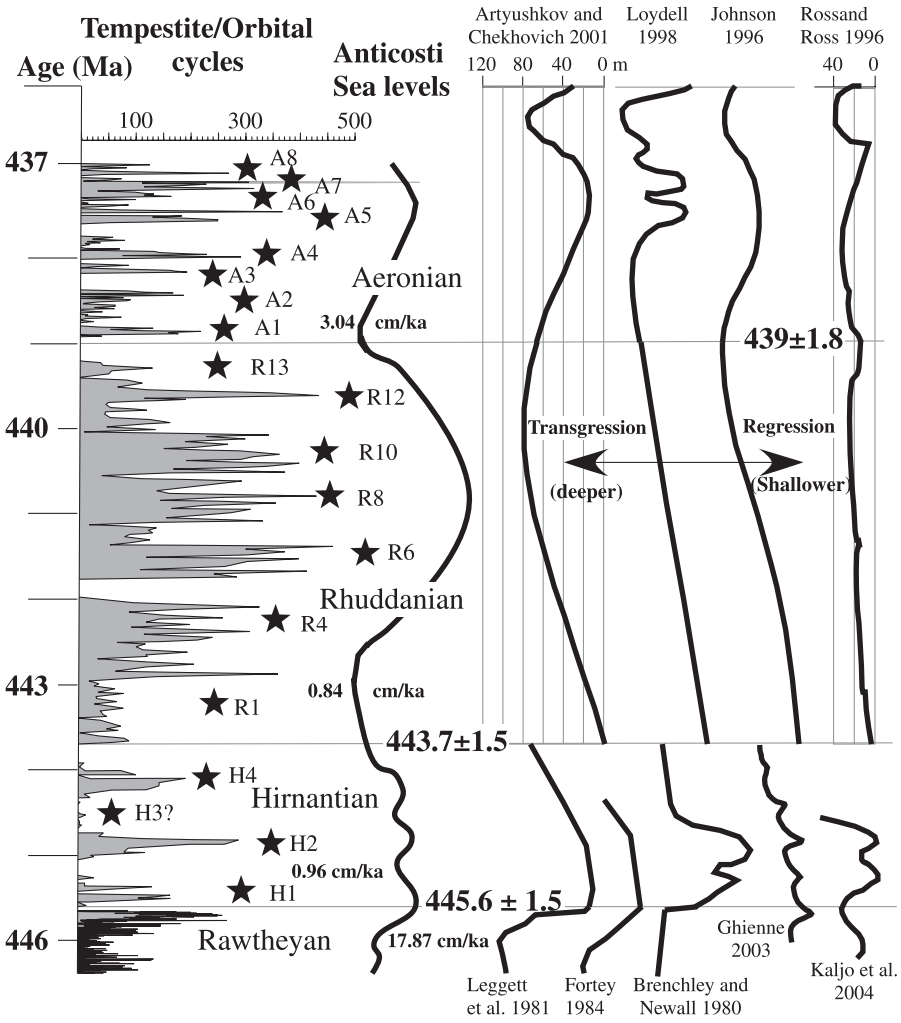

able to bypass the coastal zone and was redistributed by hurricane-driven storms across the ramp, mostly from the northeast. Small bioherms were able to develop in nearshore settings at times of falling sea level in the latest Ordovician, despite the siliciclastic input. Under fair-weather conditions, finer grained detritus may have been confined to the inner parts of the shelf by coastal boundary currents. As the basin continued to subside, the influence of siliciclastic input declined, constrained in part by development of coastal boundary currents, and larger reefs were able to develop on shoals in a mid-shelf setting.

Subsidence analysis confirms the influence of tectonic loading from the Gaspé and Miramichi regions to the south during the Taconic orogeny, with distinct intervals of thrust loading in the Caradocian and Ashgillian, and possibly the Aeronian, confirming the suggestion by Ettenson and Brett (2002) that the Taconic orogeny continued into the Silurian. Tempestite frequency analysis appears to provide a good proxy record for sea-level change or shifts in storm belt location and intensity and is not masked by subsidence rates, at least in inner shelf settings. Most significantly, it can be resolved in terms of orbital cyclicity, involving both long- and short-term obliquity. The record is subdued or obscured in very deep (>100 m) water due to the paucity of storm beds, and also in very shallow settings because of erosion or amalgamation of beds. The apparent coherence of the tempestite curves to the local sea-level curve deduced from sedimentary structures suggests that maximum 4th- and possibly 3rd-order sea-level changes were only a few tens of metres at the most (if the effect of tectonic and sediment load-induced subsidence is considered), confirming observations by Artyushkov and Chekhovich (2001) from east Siberia. Johnson et al. (1998) have used Silurian coastal topography to suggest a maximum 70 m sea-level rise during the post-Hirnantian, Rhuddanian transgressive event, and 63 m during the Aeronian transgressive event (Fig. 9). Neither of these values had been corrected for the influence of isostatic loads (cf. Long 1993*a*). As the half-life for isostatic recovery from loading is about 4400 a (Allen and Allen 1990), and given that 1 m of water will eventually depress the crust by 1.43 m (with no sedimentation), or by as much as 2.65 m if sedimentation fills all available accommodation space (Matthews 1984), then absolute sea-level changes as low as 26 and 24 m can explain apparent sea-level changes based

on both coastal topography and sedimentary structures. Comparison of weighted tempestite frequency curves from this study plotted against time (Fig. 10) show marked departure from existing sea-level models for the Late Ordovician (Brenchley and Newall 1980; Leggett et al. 1981; Fortey 1984; Ghienne 2003; Kaljo et al. 2004) and Early Silurian (Johnson 1996; Ross and Ross 1996; Loydell 1998; Artyushkov and Chekhovich 2001). The Rawtheyan segment of the Leggett et al. (1981) curve shows the best fit to the tempestite data from the Vauréal Formation. The presence of only two eustatic drops in the curves of Brenchley and Newall (1980) and Kaljo et al. (2004) may indicate that they are missing strata from the upper part of the Hirnantian glacial interval. All models allow for a major drop in sea level prior to the Ordovician–Silurian boundary. Most of the published sea-level curves for the Rhuddanian show an overall deepening trend (Fig. 10). The smoothed (3rd-order) sea-level trend from the tempestite data appears to show the opposite trend from 443 to 438 Ma. This may indicate that at times of slow subsidence (0.84 cm/ka), sediment flux from the inner shelf may have exceeded the available shallow-water accommodation space and promoted seaward progradation of facies. The regressive trend in the Aeronian reflects the predicted curves from Artyushkov and Chekhovich (2001), Johnson (1996), and possibly Loydell (1998) but is not comparable to the predicted curve of Ross and Ross (1996).

This paper demonstrates the potential use of moving bed-by-bed stratigraphic measurements both to constrain tectonic models of foreland basins and to seek out astronomical cycles in the geological record. Further detailed stratigraphic analysis of the upper Jupiter Formation and Chicotte Formation is needed to determine whether obliquity cycles influenced this part of the succession.

Acknowledgements

I thank the Natural Sciences and Engineering Research Council for funding this research under the Discovery Grants Program, and C. Mitchell, C. Brett, and M. Gibling for providing constructive comments on the manuscript.

References

Aigner, T. 1985. Storm depositional systems. Lecture Notes in Earth Sciences 3. Springer Verlag, Berlin, Germany.

Aigner, T., and Reineck, H.-E. 1982. Proximality trends in modern storm sands from Helgoland Bight (North Sea) and their implications for basin analysis. Senckenbergiana Maritime, **14**: 183–215.

Allen, J.R.L. 1982. Sedimentary structures, their character and physical basis. Vol. 2. Elsevier, Amsterdam, The Netherlands.

Allen, J.R.L. 1984. Wrinkle marks: an intertidal sedimentary structure due to aseismic soft-sediment loading. Sedimentary Geology, **41**: 75–95.

Allen, P.A., and Allen, J.R. 1990. Basin analysis, principles and applications. Blackwell Scientific Publications, Oxford, UK.

Artyushkov, E.V., and Chekhovich, P.A. 2001. The East Siberian basin in the Silurian: evidence for no large-scale sea-level changes. Earth and Planetary Science Letters, **193**: 183–196.

Baarli, B.G. 1988. Bathymetric co-ordination of proximality trends and level-bottom communities: a case study from the Lower Silurian of Norway. Palaios, **3**: 577–587.

Baarli, B.G. 1998. Silurian cycles and proximality-trend analysis of tempestite deposits. *In* Silurian cycles: linkages of dynamic stratigraphy with atmospheric, oceanic and tectonic changes. *Edited by* E. Landing and M.E. Johnson. James Hall Centennial Vol., New York State Museum Bulletin, 491, pp. 75–88.

Baldwin C.T., and Johnston, H.T. 1977. Sandstone mounds and associated facies sequences in some late Precambrian and Cambro-Ordovician inshore tidal flat lagoonal deposits. Sedimentology**,** **24**: 801–818.

Barnes, C.R. 1988. Stratigraphy and palaeontology of the Ordovician–Silurian boundary interval, Anticosti Island, Quebec. Bulletin of the British Museum of Natural History (Geology), **43**: 195–219.

Bédard, J.H. 1992. Jurassic quartz-normative tholeiite dikes from Anticosti Island, Quebec. *In* Eastern North American Mesozoic magmatism. *Edited by* J.H. Puffer and P.C. Ragland. Geological Society of America, Special Paper 268, pp. 161–167.

Berger, A., and Loutre, M.F. 1994. Astronomical forcing through geological time. *In* Orbital forcing and cyclic sequences. *Edited by* P.L. de Boer and D.G. Smith. International Association of Sedimentologists, Special Publication 19, pp. 15–24.

Brenchley, P.J., and Newall, G. 1980. A facies analysis of Upper Ordovician regressive sequences in the Oslo region, Norway—A record of glacio-eustatic changes. Palaeogeography, Palaeoclimatology and Palaeoecology, **31**: 1–38.

Brenchley, P.J., Marshal, J.D., Robertson, D.B.R., Carden, G.A.F., Meidla, T., Hints, L., and Long, D.G.F. 1994. Bathymetric and isotopic evidence for a short-lived late Ordovician glaciation in a greenhouse period. Geology, **22**: 295–298.

Brett, C.E., Boucot, A.J., and Jones, B. 1993. Absolute depths of Silurian benthic assemblages. Lethaia, **26**: 25–40.

Brunton, F.H. 1988. Silurian (Llandovery–Wenlock) patch reef complexes of the Chicotte Formation of Anticosti Island. Unpublished M.Sc. thesis, Laurentian University, Sudbury, Ontario, Canada.

Brunton, F.H., and Copper, P. 1994. Paleoecologic, temporal and spatial analysis of Early Silurian reefs of the Chicotte Formation, Anticosti Island, Quebec, Canada. Facies, **31**: 57–80.

Carden, G.A.F. 1995. Stable isotopic changes across the Ordovician–Silurian boundary. PhD thesis, University of Liverpool, Liverpool, UK.

Cheel, R.J. 1991. Grain fabric in hummocky cross-stratified storm beds: genetic implications. Journal of Sedimentary Petrology, **61**: 102–110.

Cooper, R.A., and Sadler, P.M. 2004. The Ordovician Period. *In* A geologic time scale 2004. *Edited by* F.M. Gradstein, J.G. Ogg, and A.G. Smith. Cambridge University Press, Cambridge, UK., pp. 165–187.

Copper, P. 1989. Upper Ordovician and Lower Silurian reefs of Anticosti Island, Quebec. *In* Reefs, Canada and adjacent areas. *Edited by* H.H.H. Geldsetzer, N.P.James, and G.E.Tebbutt. Canadian Society of Petroleum Geologists, Memoir, 13, pp. 271–276.

Copper, P., and Long, D.G.F. 1989. Stratigraphic revisions for a key Ordovician–Silurian boundary section, Anticosti Island, Canada. Newsletters on Stratigraphy, **21**: 59–73.

Copper, P., and Long, D.G.F. 1990. Stratigraphic revision of the Jupiter Formation. Newsletters on Stratigraphy, **23**: 11–36.

Cousineau, P.A., and Longuépée, H. 2003. Lower Paleozoic configuration of the Quebec reentrant based on improved along-strike paleogeography. Canadian Journal of Earth Sciences, **40**: 207–219.

De Boer, P.L., and Smith, D.G. 1994. Orbital forcing and cyclic sequences. International Association of Sedimentologists, Special Publication 19.

Desrochers, A. 1988. Stratigraphie de l'Ordovicien de la region de

l'archipel de Mingan. Direction Generale de la Recherche Geologique et Minerale. Ministère de l'Énergie et des Ressources Centre de Diffusion de la Geoinformation, Québec, Canada, Report MM 87-01, 70 p.

Desrochers, A. 2004. High frequency sea level fluctuations in encrinite and reefal limestones accumulating along rocky shorelines: an example from the Lower Silurian Chicotte Formation, Anticosti Island, Canada. International Geological Congress, August 2004, Florence, Italy.

Desrochers, A., and James, N.P. 1988. Early Paleozoic surface and subsurface paleokarst: Middle Ordovician carbonates, Mingan Islands, Quebec. *In* Paleokarst. *Edited by* N.P. James and P.W. Choquette. Springer-Verlag, Berlin, Germany, pp. 183–210.

Desrochers, A., Copper, P., and Long, D.G.F. 1998. Sedimentology and paleontology of Early Ordovician through Early Silurian shallow-water carbonates of the Mingan Islands and Anticosti Island. Geological Association of Canada, Mineralogical Association of Canada, Canadian Geophysical Union, Joint Annual Meeting, Québec City, Quebec, 20–26 May 1998. Field Trip B8, Guidebook.

Diecchio, R.J. 1995. Sea-level changes and correlation of Ordovician–Silurian boundary sections in Appalachian basin and Anticosti Island based on cumulative aggradation plots. *In* Ordovician Odyssey: short papers for the 7th international symposium on the Ordovician System. *Edited by* J.D. Cooper, M.L. Droser, and S.C. Finney. Pacific Section, Society for Sedimentary Geology (SEPM), Fullerton, Calif., USA, pp. 337–341.

Dott, R.H., and Bourgeois, J. 1982. Hummocky cross-stratification: significance of its variable bedding sequence. Geological Society of America, Bulletin, **93**: 663–680.

Droser, M.L., and Bottjer, D.J. 1989. Ichnofabric of sandstones deposited in high energy nearshore environments: measurements and utilization. Palaios, **4**: 598–604.

Duke, W.L. 1985. Hummocky cross-stratification, tropical hurricanes and intense winter storms. Sedimentology, **32**: 167–194.

Easthouse, K.A., and Driese, S.G. 1988. Paleobathymetry of a Silurian shelf system: application of proximality trends and trace fossil distribution. Palaios, **3**: 473–486.

Ettenson, F.R., and Brett, C.E. 2002. Stratigraphic evidence from the Appalachian Basin for continuation of the Taconic orogeny into Early Silurian time. Physics and Chemistry of the Earth, **27**: 279–288.

Fedo, C.M., and Cooper, J.D. 1990. Braided fluvial to marine transition: the basal Lower Cambrian Wood Canyon Formation, southern Marble Mountains, Mojave Desert, California. Journal of Sedimentary Petrology, **60**: 220–234.

Fortey, R.A. 1984. Global earlier Ordovician transgressions and regressions and their biological implications. Paleontological Contributions from the University of Oslo, **295**: 37–50.

Fortey, R.A., Harper, D.A.T., Ingham, J.K., Owen, A.W., and Rushton, A.W.A. 1995. A revision of Ordovician series and stages from the historical type area. Geological Magazine, **132**: 15–30.

Ghienne, J-F. 2003. Late Ordovician sedimentary environments, glacial cycles, and post-glacial transgression in the Taoudeni Basin, West Africa. Palaeogeography, Palaeoclimatology, and Palaeoecology, **189**: 117–145.

Hagadorn, J.W., and Bottjer, D.J. 1997. Wrinkle structures: microbially mediated sedimentary structures common in subtidal siliciclastic settings at the Proterozoic–Phanerozoic transition. Geology, **25**: 1047–1050.

Hovland, M. 1989. Modern analogues to middle Ordovician sedimentary mounds and washout depressions. Journal of Sedimentary Petrology, **59**: 585–589.

INRS-Pétrole. 1974. Arco-Anticosti No. 1, sedimentologic, mineralogical, bio-stratigraphical, geochemical, organic and mineral study, diagenesis and petroleum potential. Institut National de la Recherche Scientifique, Université de Québec, Sainte-Foy, Quebec, Report M.R.N. No. 7.

Jin, J., Long, D.G.F., and Copper, P. 1996. Early Silurian *Virgiana* pentamerid brachiopod community of Anticosti Island, Quebec. Palaios, **11**: 597–609.

Johnson, M.E. 1996. Stable cratonic sequences and a standard for Silurian eustasy. *In* Paleozoic sequence stratigraphy: views from the North American craton. *Edited by* B.J. Witzke, G.A. Ludvigson, and J. Day. Geological Society of America, Special Paper 306, pp. 203–221.

Johnson, M.E., Rong, J-Y., and Kershaw, S. 1998. Calibrating Silurian eustasy against the erosion and burial of coastal paleotopography. *In* Silurian cycles: linkages of dynamic stratigraphy with atmospheric, oceanic and tectonic changes. *Edited by* M.E. Johnson and E.W. Landing. James Hall Centennial Vol., New York State Museum Bulletin, 491, pp. 3–13.

Kaljo, D., Hints, L., Martma, T., Nõlvak, J., and Oraspõld, A. 2004. Late Ordovician carbon isotope trend in Estonia, its significance in stratigraphy and environmental analysis. Palaeogeography, Palaeoclimatology and Palaeoecology, **210**: 165– 185.

Kopaska-Merkel, D.C., and Grannis, J. 1990. Detailed structure of wrinkle marks. Journal of the Alabama Academy of Science, **61**: 236–243.

Koren, T.N. 1991. Evolutionary crisis of the Ashgill graptolites. *In* Advances in Ordovician geology. *Edited by* C.R. Barnes and S.H. Williams. Geological Survey of Canada, Paper 90-9, pp. 157–164.

Lavoie, D., Burden, E., and Lebel, D. 2003. Stratigraphic framework for the Cambro-Ordovician rift and passive margin successions from southern Quebec to western Newfoundland. Canadian Journal of Earth Sciences, **40**: 177–205.

Leggett, J.K., McKerrow, W.S., Cocks, L.R.M., and Rickards, R.B. 1981. Periodicity in the early Paleozoic marine realm. Journal of the Geological Society (of London), **138**: 167–176.

Long, D.G.F. 1993*a*. Limits on late Ordovician eustatic sea-level change from carbonate shelf sequences: an example from Anticosti Island, Quebec. *In* Sequence stratigraphy and facies associations. *Edited by* H.W. Posamentier, C.P. Summerhayes, B.H. Haq, and G.P. Allen. International Association of Sedimentologists, Special Publication 18, pp. 487–499.

Long, D.G.F. 1993*b*. Oxygen isotopes and event stratigraphy near the Ordovician–Silurian boundary. Palaeogeography, Palaeoclimatology, Palaeoecology, **104**: 49–59.

Long, D.G.F. 1993*c*. The Burgsvik beds, a Late Silurian storm generated sand ridge complex in southern Gotland. Geologiska Föreningens i Stockholm Förhandlingar, **115**: 299–309.

Long, D.G.F. 1996. Paleocurrents, paleodepths, and paleosubsidence along the eastern margin of Laurentia as recorded in Late Ordovician and Early Silurian carbonates of the Anticosti Platform, Quebec, Canada. James Hall symposium, Second international symposium on the Silurian System, Rochester, NY, 4–9 August 1996. Program and Abstracts, 2, p. 71.

Long, D.G.F. 1997. Seven million years of storm redistribution along the east coast of Laurentia: transport mechanisms, current systems and influence of siliciclastics on reef development in the Late Ordovician and Early Silurian carbonate ramp of Anticosti Island, Quebec, Canada. Proceedings of the 8th International Coral Reef Symposium, Panama, 2. pp. 1743–1748.

Long, D.G.F., and Copper, P. 1987*a*. Stratigraphy of the Upper Ordovician Vauréal and Ellis Bay Formations, eastern Anticosti Island. Canadian Journal of Earth Sciences, **24**: 1807–1820.

Long, D.G.F., and Copper, P. 1987*b*. Late Ordovician sand-wave complexes on Anticosti Island, Quebec: a marine tidal embayment? Canadian Journal of Earth Sciences, **24**: 1820–1832.

Long, D.G.F., and Copper, P. 1994. The Late Ordovician – Early Silurian carbonate tract of Anticosti Island, Gulf of St. Lawrence, Eastern Canada. Geological Association of Canada, Mineralogical Association of Canada, Joint Annual Meeting, Waterloo, Ontario, 20–25 May 1994. Field Trip Guidebook B4.

Loydell, D.K. 1998. Early Silurian sea-level changes. Geological Magazine, **135**: 447–471.

Malo, M. 2004. Paleogeography of the Matapédia basin in the Gaspé Appalachians: initiation of the Gaspé Belt successor basin. Canadian Journal of Earth Sciences, **41**: 533–570.

Martinsson, A. 1965. Aspects of a Middle Cambrian thanatotope on Öland. Geologiska Föreningens i Stockholm Förhandlingar, **87**: 181–230.

Matthews, R.K. 1984. Dynamic stratigraphy, an introduction to sedimentation and stratigraphy. 2nd ed. Prentice Hall, N.J., USA.

Melchin, M.J., Cooper. R.A., and Sadler, P.M. 2004. The Silurian Period. *In* A geologic time scale 2004. *Edited by* F.M. Gradstein, J.G. Ogg, and A.G. Smith. Cambridge University Press, Cambridge, UK., pp. 188–201.

Myrow, P.M., and Southard, J.B. 1991. Combined-flow model for vertical stratification sequences in shallow marine storm-deposited beds. Journal of Sedimentary Petrology, **61**: 202–210.

Myrow, P.M., and Southard, J.B. 1996. Tempestite deposition. Journal of Sedimentary Research **66**: 875–887.

Noffke, N., Gerdes, G., Klenke, T., and Krumbein, W.E. 2001. Microbially induced sedimentary structures: a new category within the classification of primary sedimentary structures. Journal of Sedimentary Research, **71**: 649–656.

Pe-Piper, G., and Piper, D.J.W. 1999. Were Jurassic tholeiitic lavas originally widespread in southeastern Canada? A test of the broad terrane hypothesis. Canadian Journal of Earth Sciences, **36**: 1509–1516.

Pruss, S., Fraiser, M., and Bottjer, D.J. 2004. Proliferation of Early Triassic wrinkle structures: implications for environmental stress following the end-Permian mass extinction. Geology, **32**: 461–464.

Pruss, S., Corsetti, F.A., and Bottjer, D.J. 2005. The unusual sedimentary record of the Early Triassic: a case study from the southwestern United States. Palaeogeography, Palaeoclimatology, Palaeoecology, **222**: 33–52.

Read, J.F. 1995. Overview of carbonate platform sequences, cycle stratigraphy and reservoirs in greenhouse and icehouse worlds. *In* Milankovitch sea level changes, cycles and reservoirs on carbonate platforms in greenhouse and icehouse worlds. *Edited by* J.F. Read, C. Kerans, and L.J. Webber. SEPM (Society for Sedimentary Geology), Short Course Notes, 35, pp. 1–102.

Reineck, H.-E. 1969. Die entstehung von runzelmarken. Natur und Museum, **99**: 386–388.

Riva, J. 1988. Graptolites at and below the Ordovician–Silurian boundary on Anticosti Island, Canada. Bulletin of the British Museum of Natural History (Geology), **43**: 221–237.

Roliff, W.A. 1968. Oil and gas exploration—Anticosti Island, Quebec. Proceedings of the Geological Association of Canada, **19**: 31–36.

Ross, C.A., and Ross, R.P. 1996. Silurian sea-level fluctuations. *In* Paleozoic sequence stratigraphy: views from the North American craton. *Edited by* B.J. Witzke, G.A. Ludvigson, and J. Day. Geological Society of America, Special Paper 306, pp. 187–192.

Sami, T. 1989. Episodic sedimentation on an early Silurian, storm dominated carbonate ramp, Anticosti Island, Quebec. Unpublished M.Sc. thesis. University of Ottawa, Ottawa, Ont., Canada.

Sami, T., and Desrochers, A. 1992. Episodic sedimentation on an early Silurian, storm dominated carbonate ramp, Becscie and Merrimack Formations, Anticosti Island, Quebec. Sedimentology, **39**: 355–381.

Seed, H.B., and Rhaman, M.S. 1978. Wave-induced pore pressure in relation to ocean floor stability of cohesionless soils. Marine Geotechnology, **3**: 123–150.

Sepkoski, J.J., Jr. 1982. Flat-pebble conglomerates, storm deposits, and the Cambrian bottom fauna. *In* Cyclic and event stratification. *Edited by* G. Einsele and A. Seilacher. Springer-Verlag, Berlin, Germany, pp. 371–385.

Stockmal, G.S., Waldron, J.W.F., and Quinlan, G.M. 1995. Flexural modelling of Paleozoic foreland basin subsidence, offshore western Newfoundland; evidence for substantial post-Taconian thrust transport. Journal of Geology, **103**: 653–671.

Sutcliffe, O.E., Dowdeswell, J.A., Whittington, R.J.,Theron, J.N., and Craig, J. 2000. Calibrating the Late Ordovician glaciation eccentricity cycles of Earth's orbit. Geology, **28**: 967–970.

Swift, D.J.P., Figueirdo, A.G., Freeland, G.L., and Oertel, G.F. 1983. Hummocky cross-stratification and megaripples: a geological double standard? Journal of Sedimentary Petrology, **53**: 1295–1317.

Underwood, C.J., Crowley, S.F., Marshall, J.D., and Brenchley, P.J. 1997. High resolution carbon isotope stratigraphy of the basal Silurian stratotype (Dob's Linn, Scotland) and its global relationship. Journal of the Geological Society (of London), **154**: 709–718.

Waldron, J.W.F., Anderson, S.D., Carwood, P.A., Goodwin, L.B., Hall, J., Jamieson, R.A., Palmer, S.E., Stockmal, G.S., and Williams, P.F. 1998. Evolution of the Appalachian Laurentian margin: Lithoprobe results in western Newfoundland. Canadian Journal of Earth Sciences, **35**: 1271–1287.

Wanless, H.R., Tedesco, L.P., and Tyrell, K.M. 1988. Production of subtidal tubular and surficial tempestites by hurricane Kate, Caicos Platform, British West Indies. Journal of Sedimentary Petrology, **58**: 739–750.

Wilde, P. 1991. Oceanography in the Ordovician. *In* Advances in Ordovician geology. *Edited by* C.R. Barnes and S.H. Williams. Geological Survey of Canada, Paper 90–9, pp. 283–298.

Yagishita, K., Arakawa, S., and Taira, A. 1992. Grain fabric of hummocky and swaley cross-stratification. Sedimentary Geology, **78**: 181–189.

Zhang, S., and Barnes, C.R. 2002. Late Ordovician–Early Silurian (Ashgillian–Llandovery) sea level curve derived from conodont community analysis, Anticosti Island, Quebec. Palaeogeography, Palaeoclimatology, Palaeoecology, **180**: 5–32.